

SCANNING TUNNELING MICROSCOPY
WITH ELECTROCHEMICAL CAPABILITIES

THESIS

Presented to the Graduate Council of
Southwest Texas State University
in Partial Fulfillment of
The Requirements

For the Degree

Master of SCIENCE

By

Paul Person, B.S.

San Marcos, Texas
May 1999

*This thesis is dedicated to my friends and loved ones for their kindness
and continuing support.*

ACKNOWLEDGEMENTS

I wish to thank Dr. Heather Galloway for her guidance, support, and patience. She has taught me too not to just read, but think and concentrate. I also extend thanks to my thesis committee members Dr. Victor E. Michalk and Dr. Ir. Wilhelmus J. Geerts for their contributions to the thesis.

I want to also recognize professors Dr. Carlos Gutierrez, Dr. William Jackson, and Dr. Donald Olson. These professors helped me discover the multitude of physics that occurs in everyday life. I thank the whole physics department for teaching me to challenge myself, not by working hard, but by working smart. Other fellow colleagues I have grown to appreciate include Kelly Fishbeck, Robert Villarreal, Yuji Yamaguchi, Kevin Wiederhold, and Anival Ayala. I wish the best for whoever will be continuing this work after my departure.

A special thanks goes out to Michael Matheaus, Charles Watts, and Nelson White for the years of friendship throughout undergraduate and graduate school. Physics with these three is not physics, but a combination of humor and unexplainable questions.

My father, my mother, and the rest of my family are the best. They provide unconditional support and love throughout my life.

May 5, 1999

TABLE OF CONTENTS

ACKNOWLEDGEMENTS	iv
LIST OF TABLES	vii
LIST OF FIGURES	viii

CHAPTER

1	INTRODUCTION	
1.1	HISTORY OF SCANNING TUNNELING MICROSCOPY	1
1.2	DEFINITION OF ELECTROCHEMICAL STM	1
2	THEORY OF SCANNING TUNNELING MICROSCOPY	
2.1	BASIC PRINCIPLES	3
2.1.1	TUNNELING	3
2.1.2	PIEZOELECTRIC MATERIAL	6
2.2	STM IMAGING	8
2.2.1	FEEDBACK LOOP	8
2.2.2	TOPOGRAPHIC METHOD	9
2.2.3	CURRENT METHOD	10
2.3	EXPERIMENTAL CONDITIONS	11
3	DESIGN CONSIDERATIONS FOR AN STM	
3.1	MECHANICAL STRUCTURE AND COMPONENTS	13
3.1.1	TIP	13
3.1.2	SCANNER	16
3.1.3	SAMPLE POSITIONER	19
3.1.4	VIBRATION ISOLATION	20
3.1.5	ELECTROMAGNETIC ISOLATION	21
3.2	CONTROL ELECTRONICS	22
3.2.1	RHK STM-100 REV. 3	22
3.2.2	DATA ACQUISITION CARD	23
3.2.3	SPM 32 SOFTWARE	23
4	DOUBLE TUBE DESIGN	
4.1	APPARATUS DESIGN	25
4.2	RHK STM-100 REV. 3 CONFIGURATION	27
4.3	SPM 32 SOFTWARE CONFIGURATION	28
4.4	SAMPLE APPROACH	28
4.5	FREQUENCY OF VIBRATION	29

5	JOHNNY WALKER DESIGN	
5.1	APPARATUS DESIGN.....	31
5.1.1	MICROSCOPE HEAD.....	31
5.1.2	MANIPULATOR.....	33
5.1.3	WIRING.....	33
5.1.4	FARADAY CAGE.....	34
5.1.5	ROTARY SWITCH.....	34
5.2	RHK STM-100 REV. 3 CONFIGURATION.....	35
5.3	SPM 32 SOFTWARE CONFIGURATION.....	35
5.4	SAMPLE APPROACH.....	35
5.5	FREQUENCY OF VIBRATION.....	36
6	EXAMPLES OF DATA AND ANALYSIS IN STM	
6.1	INSTRUMENTATION.....	38
6.2	FAST FOURIER TRANSFORMS.....	38
6.3	EXAMPLE OF GRAPHITE DATA.....	40
6.4	EXAMPLE OF METALLIC SAMPLE.....	43
7	ELECTROCHEMICAL SCANNING TUNNELING MICROSCOPY	
7.1	THEORY.....	45
7.2	ELECTROCHEMICAL CELL.....	46
7.3	APPLICATIONS/RESEARCH AREAS.....	49
8	CONCLUSIONS	
8.1	STM AND ELECTROCHEMISTRY.....	51
8.2	FUTURE CONSIDERATIONS.....	52
	APPENDIX	
	APPENDIX A.....	54
	RHK MODEL STM 100 SWITCH POSTION OPTIONS.....	54
	APPENDIX B.....	56
	SPM 32 DOUBLE TUBE CONFIGURATION FILE.....	56
	APPENDIX C.....	63
	SPM 32 JOHNNY WALKER CONFIGURATION FILE.....	63
	BIBLIOGRAPHY.....	70

LIST OF TABLES

	Page
Table 3.1	23
Table 4.1	30
Table 4.2	30
Table 5.1	34
Table 5.2	37

LIST OF FIGURES

	Page
Figure 2.1 Classical mechanical view of electron-barrier interaction.....	3
Figure 2.2 Quantum mechanical view of electron-barrier interaction.	4
Figure 2.3 Schematic of electron at energy E tunneling through a barrier.	5
Figure 2.4 Schematic of a 2-D open circuit of piezoelectric material.	6
Figure 2.5 Schematics of a 2-D section of piezoelectric material undergoing (a) contraction and (b) expansion.	7
Figure 2.6 Schematic of the gain set too high causing the tip to react too much.	8
Figure 2.7 Schematic of the gain set too low causing the tip to react too little.	9
Figure 2.8 Schematic of the gain set correctly.	9
Figure 2.9 (a) Current held constant. (b) Graph of the current vs. the x- position on the sample.	10
Figure 2.10 (a) Tip to sample distance (z) held constant. (b) Graph of the current vs. the x-position on the sample.	11
Figure 3.1 Electrochemical etching process for Tungsten tips	15
Figure 3.2 Piezoelectric Actuators: (a) Bar, (b) Tube, and (c) Stacked Disks.	16
Figure 3.3 STM Scanners: (a) Bar Tripod, (b) Tube Tripod, (c) Single Tube, and (d) Stacked Disks.	17
Figure 3.4 Piezo Tube: (a) with uniform field, (b) with stronger field on -x and +y sides.	18
Figure 3.5 Vibration Isolation Stages: (a) Coil Spring, (b) Damped Stacked Plates, and (d) Superconducting Levitation.	20
Figure 4.1 Inner piezo configuration for the double tube design.	25
Figure 4.2 Piezo configuration for the double tube design.	26

Figure 4.3 Sled with piezo and sample holder, (a) initially, (b) with voltage applied to piezo, and (c) voltage removed and sample holder slipping across the sled.	28
Figure 5.1 Head assembly of the Johnny Walker microscope.	32
Figure 5.2 Vibration isolation stage for the Johnny Walker model.....	33
Figure 6.1 Fast Fourier transform of noise imaging while in tunneling range of the sample.....	39
Figure 6.2 Fast Fourier transform of noise imaging while out of tunneling range of the sample.	40
Figure 6.3 Atomic placement in hexagonal graphite structure.....	40
Figure 6.4 Raw graphite images taken with the double tube design, one in the +x direction and the other in the -x direction.....	41
Figure 6.5 Graphite image after image enhancement.	41
Figure 6.6 Fast Fourier transform performed on a graphite image.....	42
Figure 6.7 Line scan across a graphite sample.....	42
Figure 6.8 Raw silver image taken with the double tube design.....	43
Figure 6.9 Line scan across a silver sample.	43
Figure 6.10 A 3-D rotated image of a silver sample.	44
Figure 7.1 Two-dimensional side view of an electrochemical cell.	47
Figure 7.2 Two-dimensional side view of an electrochemical cell.	48
Figure 7.3 Johnny Walker Microscope with the addition of an electrochemical cell.	49

CHAPTER 1

INTRODUCTION

1.1 HISTORY OF SCANNING TUNNELING MICROSCOPY

In 1982 at IBM's Zurich Lab, Dr. Gerd Binnig and Dr. Heinrich Rohrer demonstrated well-controlled vacuum tunneling in their first step towards the development of Scanning Tunneling Microscopy (STM). [1] They used a piezoelectric driver to accurately control the height of a metal tip above a conductive surface, while measuring the current between them. This confirmed the expected exponential behavior of a tunneling current. Tunneling experiments before these were largely restricted to tunneling through a static barrier, consisting of a layer of oxide sandwiched between metal electrodes. Today, STM experiments can be performed in a variety of environments: air, inert gas, ultrahigh vacuum, or even liquids, as in electrochemical measurements.

1.2 DEFINITION OF ELECTROCHEMICAL STM

Electrochemical Scanning Tunneling Microscopy (ESTM) was designed to image a sample while an electrochemical reaction occurred. An ESTM, like the STM, raster scans the tip across the surface of the

sample (working electrode), while recording the changes in topography. Submersing the sample in a solution increases the difficulty due to the possibility of background current through the solution. The tunneling current is recorded in the same manner as ambient or vacuum STM. The electrochemical reaction causes a change in the surface structure of the sample. The difference between images reflects the alteration in composition and structure of the sample. ESTM has numerous other abilities, which proves to be useful in studying processes such as metal deposition, surface anodization, nanolithography, and atomic manipulation. [2-9]

CHAPTER 2

THEORY OF SCANNING TUNNELING MICROSCOPY

2.1 BASIC PRINCIPLES

2.1.1 TUNNELING

In one-dimensional classical mechanics, an electron with energy E moving in the z -direction in a potential $U(z)$ is described by the energy equation; $\frac{p_z^2}{2m} + U(z) = E$. In regions where the electron's energy is greater than the potential barrier, i.e. $E > U(z)$, the electron has enough energy to transverse the barrier with momentum p_z . On the other hand, if the energy of the electron is less than the potential of the barrier,

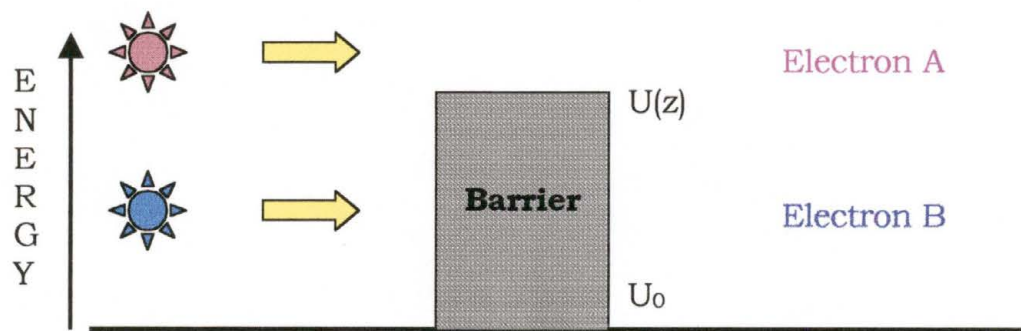


Figure 2.1 Classical mechanical view of electron-barrier interaction. Electron A has enough energy to cross the barrier. Electron B does not have enough energy to cross the barrier and is reflected.

i.e. $E < U(z)$, the electron cannot penetrate into this region and will bounce back as seen in Fig. 2.1.

In one-dimensional quantum mechanics, the state of the same electron is described by a wave function $\psi(z)$, which satisfies Schrodinger's equation,

$$-\frac{\hbar^2}{2m} \frac{d^2}{dz^2} \psi(z) + U(z)\psi(z) = E\psi(z). \quad [10]$$

In the classically allowed region for which $E > U(z)$, the wave function solutions are $\psi(z) = \psi(0)e^{\pm ikz}$, where $k = \sqrt{\frac{2m(E-U)}{\hbar^2}}$ is the wave number.

In the classically forbidden region, $U > E(z)$, the wave function solutions are $\psi(z) = \psi(0)e^{\pm\kappa z}$, where $\kappa = \sqrt{\frac{2m(U-E)}{\hbar^2}}$ is the decay constant, as seen in

Fig. 2.2. If the potential barrier is only moderately high and relatively narrow, the electron wave may continue on the opposite side of the

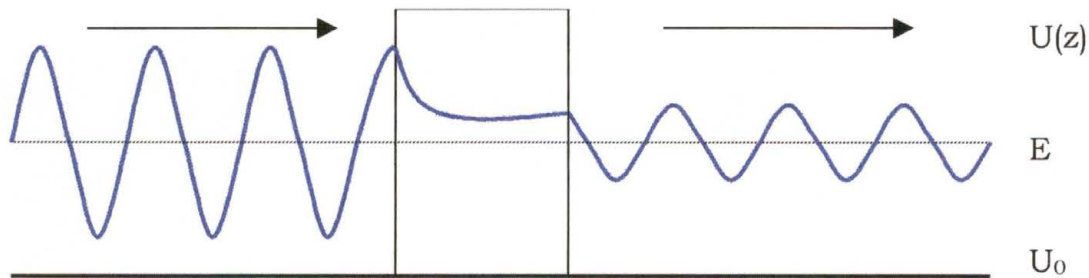


Figure 2.2 Quantum mechanical view of electron at energy E tunneling through a barrier of potential $U(z)$. Notice the exponential decay in the barrier region.

barrier. If the electron crosses the barrier, it will undergo a change in amplitude, but not a change in frequency. Therefore, the electron will have a nonzero probability to penetrate the barrier. The barrier height from E to $U(z)$ is analogous to the average work function of the tip material and the sample in a real tunneling experiment. The electron transmission probability is given by $T = \frac{(\Psi^* \Psi)_{transmitted}}{(\Psi^* \Psi)_{incident}}$, where incident means the electron before tunneling and transmitted means the electron after tunneling. In a barrier of width L and height U , the transmission probability is given by

$$T(E) = \left\{ 1 + \frac{1}{4} \left[\frac{U^2}{E(U-E)} \right] \sinh^2 \kappa L \right\}^{-1}. \quad [11]$$

Figure 2.3 depicts the situation for if an electric potential is applied between the tip and the surface of a sample. In this wave picture, the

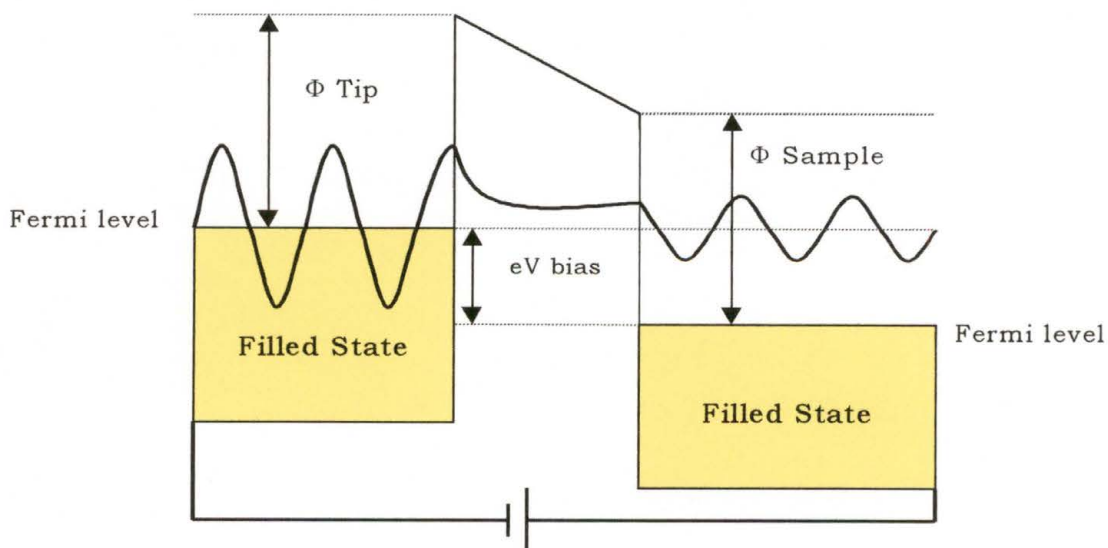


Figure 2.3 Schematic of electron at energy E tunneling through a barrier.

sample is biased relative to the tip, which gives the barrier a trapezoidal shape. The shift in the Fermi levels allows the tip to have filled states at the same energy level that the sample has unfilled states. Electrons in states below the Fermi level on the negative side (tip) tunnel into empty states or "holes" that are above the Fermi level on the positive side (sample). Other electrons will not contribute either because there are no electrons to tunnel at the higher energy, or because of the Pauli exclusion principle at lower energy. More complex calculations have shown that it is the states nearest the Fermi level that contribute to most to the tunneling current.

2.1.2 PIEZOELECTRIC MATERIAL

Material that has the ability to expand and contract when a voltage is applied to it is referred to as piezoelectric material. The most commonly used type of this material for Scanning Tunneling Microscopes is Lead Zirconate Titanate (PZT). This material is an insulator that

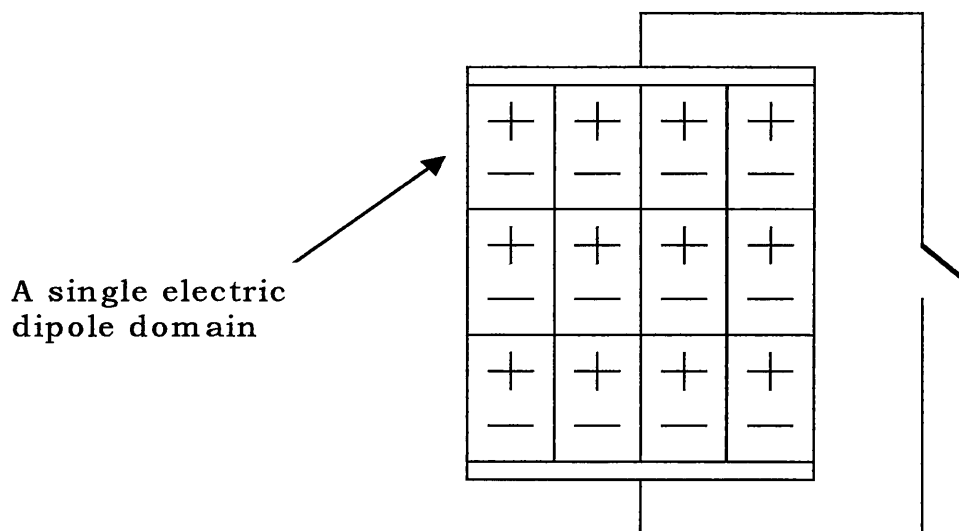


Figure 2.4 Schematic of a 2-D open circuit of piezoelectric material.

contains electric dipole domains, as shown in Fig. 2.4. The piezoelectric material is coated with nickel to create large surface electrodes. By applying a potential difference across these electrodes, an electric field is created that interacts with the dipoles of the PZT material. These domains expand or contract depending upon the direction of the applied electric field, see Fig. 2.5. The magnitude of the electric field applied controls the amount of the expansion or contraction.

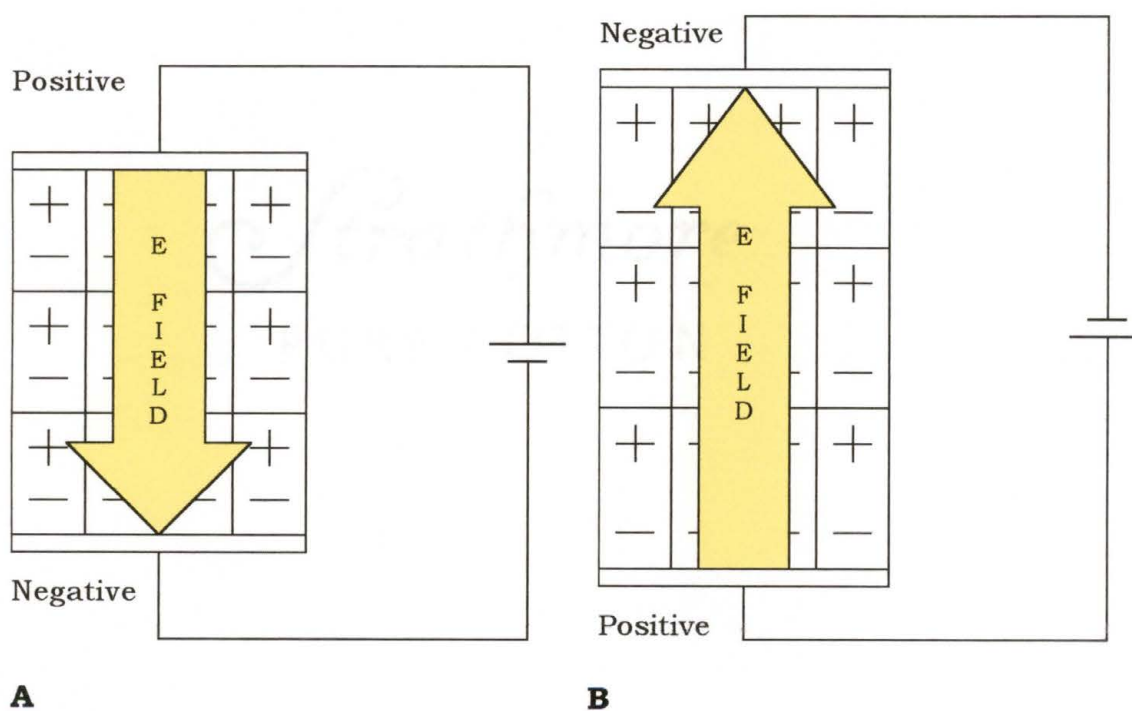


Figure 2.5 Schematics of a 2-D section of piezoelectric material undergoing A) contraction and B) expansion.

2.2 STM IMAGING

2.2.1 FEEDBACK LOOP

During operation of the STM, a sharp metal tip is brought close enough to the surface of the sample that electrons can quantum mechanically tunnel through the barrier between the tip and sample. The tunneling current is extremely sensitive to the gap width. In fact, the current drops by approximately an order of magnitude for every angstrom of distance increase between the electrodes. These small separations ($\sim 5\text{-}20\text{\AA}$) require precise control of the positions of the electrodes and that vibrations be limited to much less than an angstrom. Electric drivers made from piezoelectric material can control the position of the tip in three dimensions. The tip is scanned in two lateral dimensions with a piezoelectric driver, while at the same time the piezoelectric driver is used to adjust the height of the tip. A feedback circuit constantly adjusts the height or current depending upon the method used. Two primary components of the feedback loop are the gain and the time constant. These two control how quickly the feedback loop reacts to a change in

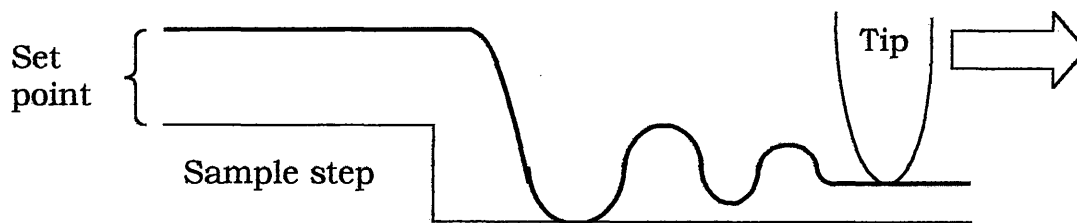


Figure 2.6 Schematic of the gain set too high causing the tip to react too much.

topography. Therefore, if the feedback loop responds too much, it can cause the tip to crash into the sample, see Fig 2.6. And naturally if the feedback responds too slowly, it can cause the tip to not adjust enough, missing some features altogether, see Fig 2.7.

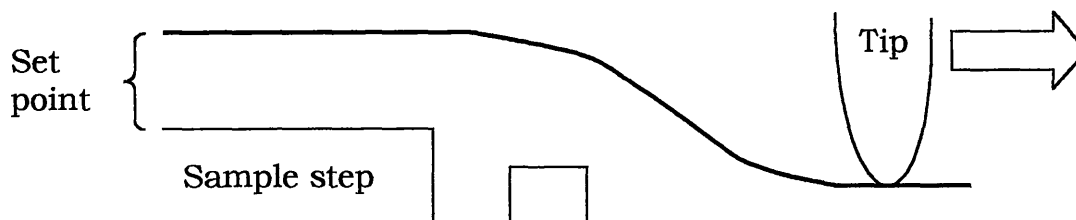


Figure 2.7 Schematic of the gain set too low causing the tip to react too little.

Figure 2.8 depicts the gain and the time constant set accurately. The path of the tip resembles the topography of the sample. The geometry of the tip, i.e. broadness, affects its ability to distinguish sharp images.

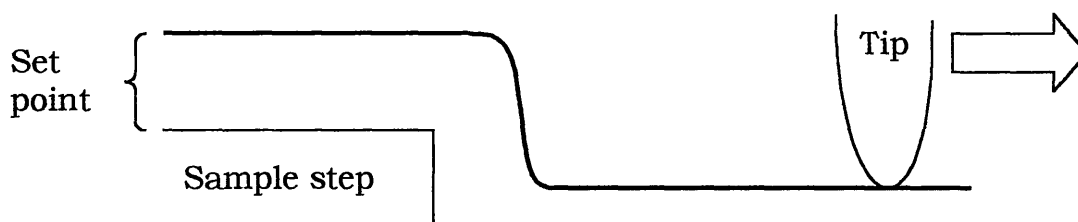


Figure 2.8 Schematic of the gain set correctly, note the path of the tip resembles the contour of the sample, although tip shape still effects the image.

2.2.2 TOPOGRAPHIC METHOD

This method of imaging maximizes the use of the feedback loop in order to adjust the tip height to keep the current constant. The path of

the tip is recorded as a contour of constant electronic density across the sample. The height of this contour can be inferred directly from the voltage supplied to the piezoelectric drivers. This method, commonly called the topographic method, is primarily used for rough metallic samples in our double tube design system.

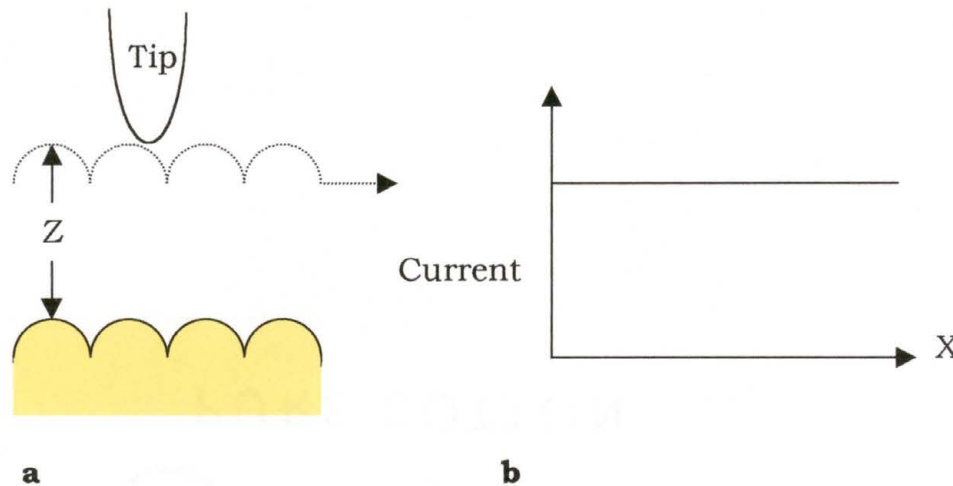


Figure 2.9 a) Current held constant. b) Graph of the current vs. the X position on the sample.

2.2.3 CURRENT METHOD

Another method of scanning is called the constant height or current method. In the current method, minimal feedback is used for the height, so the height remains relatively constant above the average surface. The tip is scanned across the sample at a relatively quick pace to also minimize the time available for the feedback to respond. The change in current is recorded as the electronic density across the sample. This method of holding the tip in position is effective on atomically flat samples, such as graphite.

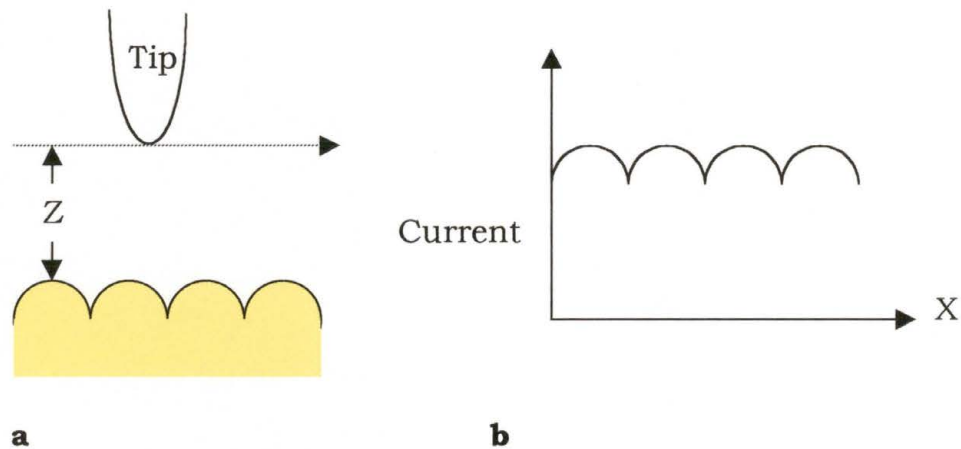


Figure 2.10 a) Tip to sample distance (Z) held constant. b) Graph of the current vs. the X position on the sample.

Another method of imaging is modulating the tip height slightly and measuring the resulting modulation of the current. This yields an image in which the local variations of the barrier height reflect the differences in electronic structure rather than topography.

2.3 EXPERIMENTAL CONDITIONS

Scanning Tunneling Microscopy can be performed in a variety of environments. Two possible environments for STM operation are Ambient-STM used for inert samples and UHV-STM (ultra high vacuum) for clean samples. Although the design concepts of the two instruments are quite similar, the construction and operation of the Ambient-STM is simpler. Acoustic coupling through components is always present in the Ambient-STM and UHV-STM, but Ambient-STM, with its compact and rigid form, is less sensitive to mechanical vibrations. The UHV-STM contains devices for mounting and changing the tip and sample, which can reduce the mechanical rigidity of the microscope and lower the

mechanical resonant frequencies. The systems for isolating the vibrations are more complex in the UHV-STM system. The design of the UHV-STM system is further complicated by the bakeout (drying the chamber) that is required for outgassing the entire vacuum system, since it requires heating the entire microscope. Also since the surface is affected by contaminants from the ambient atmosphere, it is often desirable that the sample be cleaned by heating it to a very high temperature.

CHAPTER 3

DESIGN CONSIDERATIONS FOR STM

3.1 MECHANICAL STRUCTURE AND COMPONENTS

There are a diverse number of designs for scanning tunneling microscopes, but only a few achieve respectable atomic resolution. The exacting tolerance of instruments with atomic resolution places a number of constraints on the design. The design and structure of the STM seems simple, but several aspects have proven difficult to control. Low frequency vibrations, small thermal drifts, and electrical noise are major obstacles that must be overcome to insure accurate placement of the tip. The spacing between the tip and the sample must be controlled with an accuracy of ~ 0.2 angstroms for resolving atoms on graphite and as small as ~ 0.001 angstroms for atomic resolution on flat metallic surfaces. Bringing the tip within tunneling range and scanning the tip in a raster pattern (back and forth, row by row), also places constraints on the design.

3.1.1 TIP

The tunneling tip is the most important part of the STM. The geometry and chemical composition of the tip affects the topographic and

spectroscopic measurements. It is possible to make metal tips with a radius of curvature of a few hundred angstroms, but not much less. The tunneling current, however, is so sensitive to distance that most of the current will travel to the closest atom on the surface. It is generally assumed that the best images result from tunneling from one single atom or a group of two or three atoms on the tip. The typical tip to sample separations are on the order of 6-15 angstroms, nucleus to nucleus. Naturally the probability of there being one atom at the tip increases with the decrease in the radius of the tip. There is also the possibility that the protruding atom on the tip is nonmetallic, which will display a different image due to the electronic structure of the tip-sample combination. This nonmetallic atom or atoms reduces the tunneling current, which forces the tip to get closer to the sample. In some cases, the nonmetallic atom may cause the tip to touch the sample.

The most common types of STM tips are electrochemically etched tungsten wires and cut or etched Pt-Rh wires. The tungsten tips are often used for the UHV-STM, where oxidation is not a factor. There are several steps to preparing sharp and "clean" tungsten tips. Tungsten tips are first electrochemically etched using 10% potassium hydroxide solution with 10-20V AC bias to etch 0.2-0.5 mm diameter tungsten wire, see Fig. 3.1. A typical current in the process is 2 to 3 amps. [12] The sides of the wire will etch quicker causing the wire to "neck" into a sharp tip. Tungsten tips made in this method will have a "wet" oxide

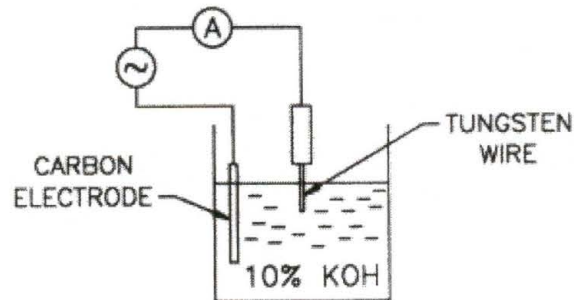


Fig. 3.1 Electrochemical etching process for Tungsten tips. [12]

layer over them. The oxide layer will cause the image quality to be poor and may cause the feedback loop to overcorrect and crash into the sample. This crash will remove the oxide layer and leave a tip in good enough shape to obtain decent imaging results. Less damaging methods to remove the oxide layer are ion milling, annealing, and field evaporation. The preferred method depends on the nature of the sample and the instrumentation available.

Pt-Rh tips are utilized in Ambient-STM because they do not oxidize in air. Pt alloy tips can be made by etching a wire (similar to the tungsten tip for UHV) or simply cut off a piece of wire. At first one would think that just cutting off a piece of wire would leave a tip that is too blunt. At the site of the cut, there still must be an atom that protrudes more than the others do. Again, occasionally a non-metallic atom could be protruding on the tip. Due to the ease of replacement, the tip may be crashed to remove the non-metallic atom.

3.1.2 SCANNER

The movement of the tip across a sample is known as scanning the sample. Scan sizes can range from zero (noise measurements) to microns of the sample. The available voltage limits the maximum displacement of the length of the piezoelectric material. Furthermore, in higher fields, the length displacement will become non-linear.

The scanner is the device that moves the tunneling tip across the sample surface and controls the tip-sample separation. The requirements of a good scanner are high resolution, orthogonality, linearity, and mechanical rigidity. Scanners made from piezoelectric actuators meet these design requirements. There are three types of piezoelectric actuators: the bar, the tube, and the stacked disks, as shown in Fig. 3.2. The bar and the tube are used in the lateral

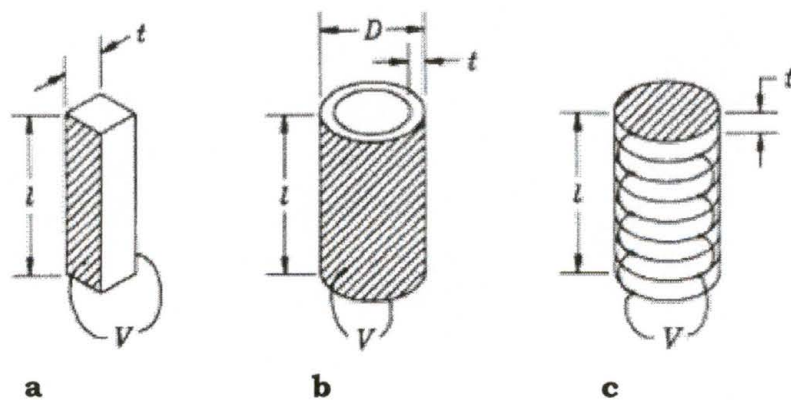


Fig. 3.2 Piezoelectric Actuators: a) Bar, b) Tube, and c) Stacked Disks. [13]

mode (displacement is perpendicular to the applied electric field). The stacked disks are used in parallel mode (displacement is in the same direction as the applied electric field). Four typical STM scanners are the bar tripod, tube tripod, single tube, and the stacked disks with mechanical amplifier, shown in figure 3.3. The tripod scanner with

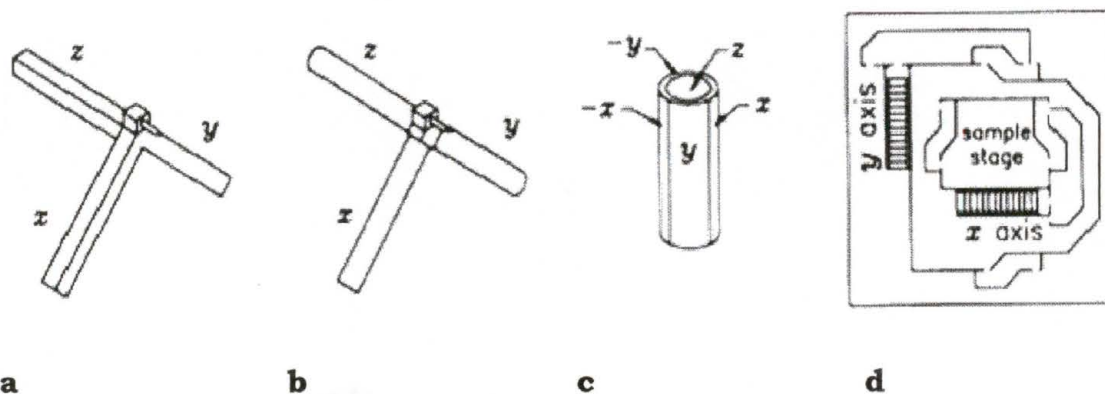


Fig. 3.3 STM Scanners: a) Bar Tripod, b) Tube Tripod, c) Single Tube, and d) Stacked Disks. [14]

three piezoelectric ceramic bars was the first type used in STM. It has reasonably high resonant frequency, relatively low sensitivity, and is reasonably orthogonal. The high resonant frequency enables the scanner to limit the amount of coupling to the lower surrounding noise frequencies. The tripod scanner with three piezoelectric tubes has a higher sensitivity and can be driven with low voltage, integrated operational amplifiers for scans of a few thousand angstroms. Scanners made with stacked piezoelectric disks coupled with mechanical amplifiers are best suited for scanning large objects over large areas (hundreds of microns) and have lower mechanical resonant frequencies.

The piezoelectric tube scanner is the most popular and the scanner used here at SWTSU, due to its compact and simple structure, high sensitivity, and high resonant frequency. This scanner has the outside electrode split into four quadrants of equal area. Lateral motion can be achieved by applying a voltage on individual electrode quadrants. For example, we apply a higher field across one quadrant and a lower field

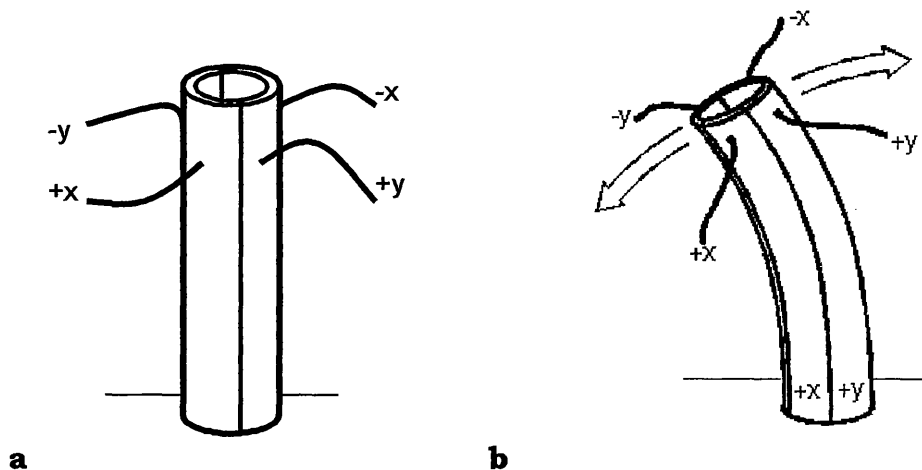


Figure 3.4 Piezo tube a) with uniform field, b) with stronger field on -x and +y sides.

across the quadrant directly across from it. The quadrant in the higher field will expand more than the one in the lower electric field. This increase in expansion on one side of tube will enable it to curve towards the side. If we slowly alter the difference between the two sides and eventually make the field on the other side larger, we will have completed a line scan.

3.1.3 SAMPLE POSITIONER

The sample positioner brings the tip close to the sample in the STM. The positioner needs to be able to retract far enough to allow the exchange of samples and be able to return to within scanning range of the piezo (z-axis). To simplify the sample approach procedure, a computer can be used to step the sample a small distance toward the tip, with the tip fully extended. After each step the current is measured to see if it is within scanning range. There are many important factors to consider when selecting a sample positioner. Examples of these are reliability of the mechanism, the geometry and rigidity of the device for certain shapes and sizes, and the speed of the approach mechanism if frequent approaches are made. These positioners are divided into three categories: screw, clamp-step, and the stick-slip. In the screw category, the devices turn by either a stepper motor mounted on the microscope or with an external motor, or by hand using a retractable shaft. This method is unfavorable in UHV-STM, due to the residues left after prolonged use; i.e. oil and metal fragments. In the clamp-step category, the devices “walk” like an inchworm: clamping one foot to a base, expanding the body, clamping the other foot to the base while releasing the first foot, and then contracting the body, usually up and down a ramp. The stick-slip or inertia devices have a sample holder resting on a plate held by a piezoelectric, which moves the sample horizontally, and

then the piezoelectric quickly retracts so that the sample slips across the base.

3.1.4 VIBRATION ISOLATION

The resolution and the sensitivity of a scanning tunneling microscope require isolation from vibrations. The vibration isolation stage provides protection from outside vibrations. Some possible methods of vibration isolation stages used in STM are damped coil spring suspension, dampers between stacked plates, and superconducting levitation, shown in figure 3.5. The superconducting levitation is

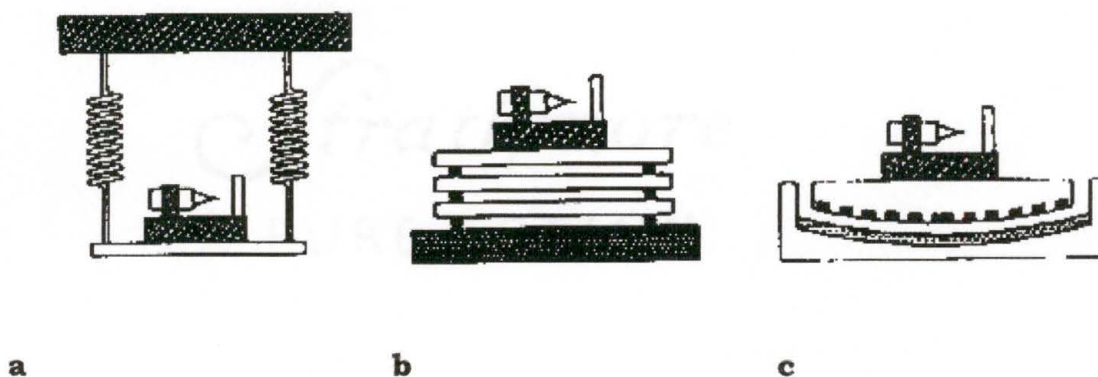


Fig. 3.5 Vibration Isolation Stages: a) Coil Spring, b) Damped Stacked Plates, and c) Superconducting Levitation. [15]

much more effective, but also more delicate and complicated. The stacked plates system and the coil spring system are easier to construct and manipulate.

Vibration isolation here in the lab at SWTSU begins with an isolated concrete floor, which limits the vibrations from the building structure. Next, the microscopes sit on air tables to limit the vibrations

from movement inside the lab. The air tables reduce low frequency vibrations (approximately 5 Hz to 20 Hz range). The double tube design (chapter 4) is hung from springs, as seen in figure 3.5, but the spring assembly has legs that are submerged in sand for additional vibration isolation. The Johnny Walker design uses the damped stacked plates, as seen in figure 3.5. The stacked plates reduce noise in the range of tens of Hz to 1kHz. Acoustical noise in the lab is reduced by the Faraday cage of the microscope, but by no means “sealed out”. So, conversations should be kept to a minimum.

3.1.5 ELECTROMAGNETIC ISOLATION

The resolution and the sensitivity of STM also requires isolation from electronic noise. This electronic noise is due to oscillating electromagnetic fields occurring in the surroundings of the STM. The noise introduced occurs in the STM tip and poorly shielded wires. The Faraday cage is meant to shield the STM from external electromagnetic fields that radiate from fluorescent light bulbs, other equipment cables, and computer monitors. It is possible to do a Fast Fourier Transform on the tunneling current signal and isolate the frequency at which both electrical and mechanical periodic noise is generated. The most common type of electrical noise is around 60Hz or harmonics of 60Hz. Other frequencies to note are monitor refresh rates, scan rates, and data acquisition sampling rates.

3.2 CONTROL ELECTRONICS

The need to control an STM dictates the use of electronics capable of measuring and of a nanoamp. The basic electronics necessary to achieve this are the preamplifier electronics, feedback electronics, scan control electronics, and computer interface for data acquisition. The current-to-voltage preamplifier is used to detect the tunneling current and amplify it in order to limit the effects of interference and noise. In a typical STM application, the tunneling bias is of the order of mV to few V and the tunneling current is of the order of 0.1-5 nA. The feedback circuit is built using operational amplifiers. The circuit starts with the output from the current preamplifier, and converts the current to a voltage. The voltage is subtracted from the reference voltage setting to obtain the error signal. The error signal is then processed by the loop filter and amplified for adjusting the tunneling gap spacing.

3.2.1 RHK STM-100 REV. 3

The control electronics used here at SWTSU is the RHK STM-100 REV. 3. The electronics allow the user to set the desired parameters at which the microscope will operate. Such parameters include scan size, image location on the sample, tunneling current, bias applied to sample, scan rate, gain/time constant, and the Z position offset.

The RHK STM-100 REV. 3 is configured with 10 circuit boards that control the outputs of the electronics. The functions of the 10 circuit boards can be seen in Table 3.1.

Board	Function
1	Z offset control
2	bias supply
3	log amplifier
4	integrator
5	Z position driver
6	X-Y interface
7&8	scan generator
9	differential X-Y scan
10	differential X-Y offset

Table 3.1 Functions of the 10 circuit boards in the RHK.

3.2.2 DATA ACQUISITION CARD

The data acquisition card (DAQ), used to interface the computer and the RHK electronics, is a Data Translations DT2821-PGH.

3.2.3 SPM 32 SOFTWARE

The operating system used for data acquisition and electronics control is SPM-32, which was designed by D.F. Ogletree of Lawrence Berkley National Laboratory. SPM-32 allows the user to alter the motion per volt applied to piezos, change the tunneling current value for which the feedback loop stops an approach, change the approach and retract "speeds" and their waveforms, and re-calibration of the x and y distortion of images. The SPM-32 also offers the user a variety of image processing techniques. Examples of these techniques include Fast Fourier Transforms, 3-D Rotations, Smoothing, Offset and Scan Subtracts. The software also has a STM status menu that relays the scan area, scan

speed, bias applied to sample, tunneling current, and the Z position of the tip.

It is possible to operate an STM without any computer interface and control, but as the applications become more complex and digital image processing becomes more useful for both image distortion correction and data analysis, a computer interface quickly becomes a necessity.

CHAPTER 4

DOUBLE TUBE DESIGN

4.1 APPARATUS DESIGN

The double tube design of a Scanning Tunneling Microscope is a horizontal model. This means that the tip is horizontal and the sample is mounted vertically on the sample holder. This design contains two piezo electric tubes, one for the tip and the other for the sample. The piezos are configured such that the tip piezo, which is much smaller, is mounted inside the sample piezo. The tip piezo and tip are assembled by taking a syringe needle and inserting it through one end. A piece of macor is glued on the tip end to keep the needle from resting against the

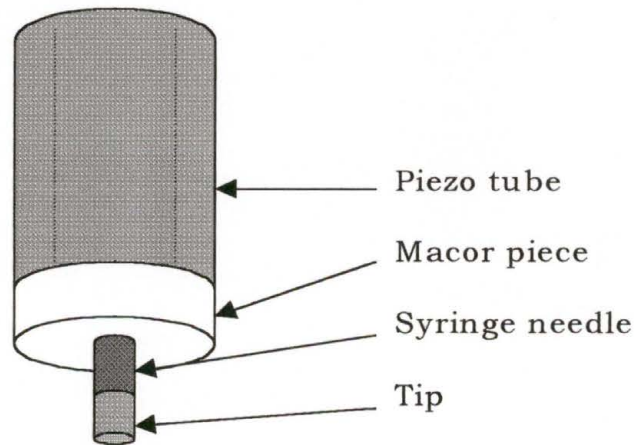


Figure 4.1 Inner piezo configuration for the double tube design.

inside of the piezo tube. On the other end a 0.004" diameter copper wire is attached to the syringe needle by sanding off the wire's insulation and using silver paste to adhere it to the needle. The 0.004" diameter copper wires that go to the piezo quadrants and the inner cylinder of the piezo tube are sanded to remove insulation from the ends and soldered to create electrical contact. The piezo is then mounted against an aluminum backing plate with holes to feed the wires through. This piezo tube has a 0.100" circumferential band on the end that connects to the aluminum plate; this eliminates grounding of the piezo electrodes. The outer or sample tube is attached to a "sled" that the sample holder will

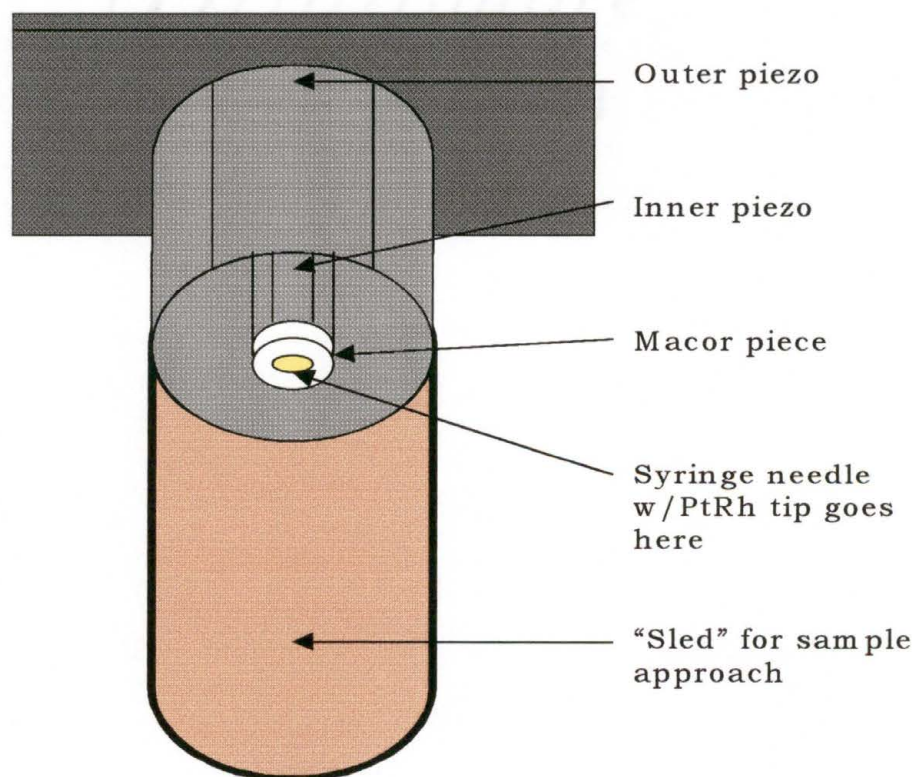


Figure 4.2 Piezo configuration for the double tube design.

ride on. The 0.004" diameter copper wire is soldered to the piezo quadrants and the inner tube. The tube is attached to the backing plate over the tip piezo. The "sled" has two gold foils attached to the inside with wires attached to them to apply a bias voltage to the sample. This whole assembly is suspended in a Faraday cage with four springs for electromagnetic and vibration isolation. All the wires are attached to insulated BNC connectors on the Faraday cage. The Faraday cage is made of a cubic aluminum frame. To eliminate electromagnetic radiation through the plexiglass, a copper mesh was glued to the insides of the plexiglass to ensure its contact with the aluminum frame. Then BNC cables are used to connect the BNC connectors to the RHK control electronics.

4.2 RHK STM-100 REV. 3 CONFIGURATION

For the double tube design the RHK STM-100 REV. 3 control electronics is configured such that:

- a) the Z offset is fed through the inertial input
- b) the Z offset knobs control the voltage at the Z offset output
- c) the Z signal is not added to X-Y scan piezos
- d) the Z offset is not added to X-Y offset piezos

Boards 1, 6, 9, and 10 of the RHK are equipped with switches that can alter the outputs of the electronics. See Appendix A for the functions of each of the switches.

4.3 SPM 32 SOFTWARE CONFIGURATION

The SPM 32 software allows the user to create a profile for an individual microscope so that the user does not have to adjust the parameters that differ between several microscopes. Parameters that differ between microscopes are the scan head type, x, y, and z motion per piezo volt, and x, y, and z offset per piezo volt. See Appendix B for the parameter file for the double tube design.

4.4 SAMPLE APPROACH

The sample approach method used by the double tube design is called the stick slip method or inertia method. The stick slip method involves applying a voltage to a piezo, then quickly removing the applied voltage. On an oscilloscope this is a saw-tooth signal. In the double

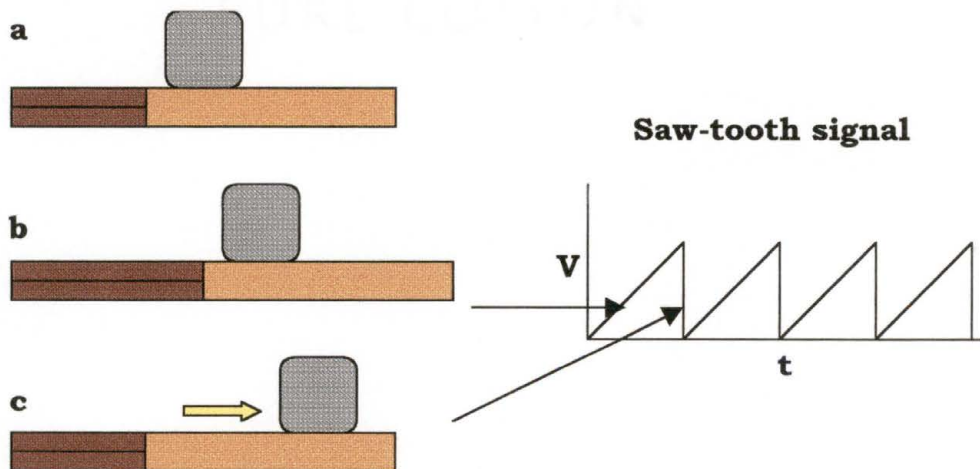


Figure 4.3 Sled with piezo and sample holder, a) initially, b) with voltage applied to piezo, and c) voltage removed and sample holder slipping across sled.

tube design there is a “sled” with a piezo attached to one end and a place for the sample holder to sit at the other end. The piezo expands or contracts depending upon the desired direction and then the piezoelectric quickly returns to its original length. This movement of the piezo and “sled” causes the sample to slip across the “sled” surface. This slipping is repeated until the sample is brought into tunneling range with the tip.

4.5 FREQUENCY OF VIBRATION

The vibrations of the tip assembly in Fig. 4.2 can be calculated to give an estimate of what resonance frequencies to expect under operation. We assume the backing plate of the piezos to be stationary to simplify the calculation. The inner and outer piezos will have independent and combined frequencies, so their frequencies are calculated individually. We call the mass of each assembly (M) and the spring constant (K) of each piezo. The spring constant (K) must be broken down into K_{\perp} for bending motions and K_{\parallel} for stretching motions.

The equations for the spring constants are $K_{\perp} = \frac{3\pi}{64} E \frac{D^4 - d^4}{L^3}$ and

$K_{\parallel} = \frac{\pi}{4} E \frac{D^2 - d^2}{L}$, where D is the outer diameter, d is the inner diameter,

L is the length, and E is the elastic modulus of the piezo. [16]

The dimensions of the inner piezo tube for the double tube microscope are L=12.70mm, D=12.70mm, and d=9.525mm. The dimensions of the outer tube are L=12.7mm, D=22.225mm, and

$d=19.05\text{mm}$. The elastic modulus of the piezo tubes is $E=6.1 \times 10^{10} \text{ N/m}^2$. The resulting spring constants for the inner and outer piezos are shown in Table 4.1.

Spring Constant	Inner Piezo	Outer Piezo
Bending motion (K_{\perp})	$7.80 \times 10^7 \text{ N/m}$	$4.92 \times 10^8 \text{ N/m}$
Stretching motion (K_{\parallel})	$2.66 \times 10^8 \text{ N/m}$	$4.94 \times 10^8 \text{ N/m}$

Table 4.1 Spring constants for piezos of double tube design.

The horizontal resonant frequency is found by using the equation

$$f_H = \frac{1}{2\pi} \sqrt{\frac{K_{\perp}}{M}}. \text{ The vertical resonant frequency is found by using the}$$

$$\text{equation } f_V = \frac{1}{2\pi} \sqrt{\frac{K_{\parallel}}{M}}. \text{ The weight of the inner piezo assembly is}$$

approximately $5.0 \times 10^{-4} \text{ kg}$ and the outer assembly is approximately

$6.0 \times 10^{-3} \text{ kg}$. The resulting frequencies are listed in Table 4.2.

Inner horizontal resonance frequency	f_{IH}	63kHz
Inner vertical resonance frequency	f_{IV}	116kHz
Outer horizontal resonance frequency	f_{OH}	1kHz
Outer vertical resonance frequency	f_{OV}	1kHz
Combined horizontal resonance frequency	f_{CIH}	32kHz
Combined vertical resonance frequency	f_{COV}	58kHz

Table 4.2 Resonance frequencies of the double tube design.

These are only estimations of noise frequencies to be aware of when imaging.

CHAPTER 5

JOHNNY WALKER DESIGN

5.1 APPARATUS DESIGN

5.1.1 MICROSCOPE HEAD

The Johnny Walker design of a Scanning Tunneling Microscope is a vertical model. This means that the tip is vertical and the sample is mounted horizontally on the sample holder. This vertical tip design is desirable in that it enables the sample to be submerged in liquids for electrochemical measurements. This design contains four identical piezoelectric tubes, one for the tip and the other three for positioning the head over the sample. The piezos are configured such that the tip is mounted in the center and the other three are used as legs in a tripod configuration, as seen in figure 5.1. The tip piezo and tip are assembled using the same method utilized on the double tube design. On the other end a 0.001" diameter copper wire is attached to the syringe needle by very carefully sanding off the wire's insulation and using silver paste to adhere it to the needle. The 0.001" diameter copper wires that go to the piezo quadrants and the inner cylinder of the tube are sanded on the ends and soldered to create an electrical contact.

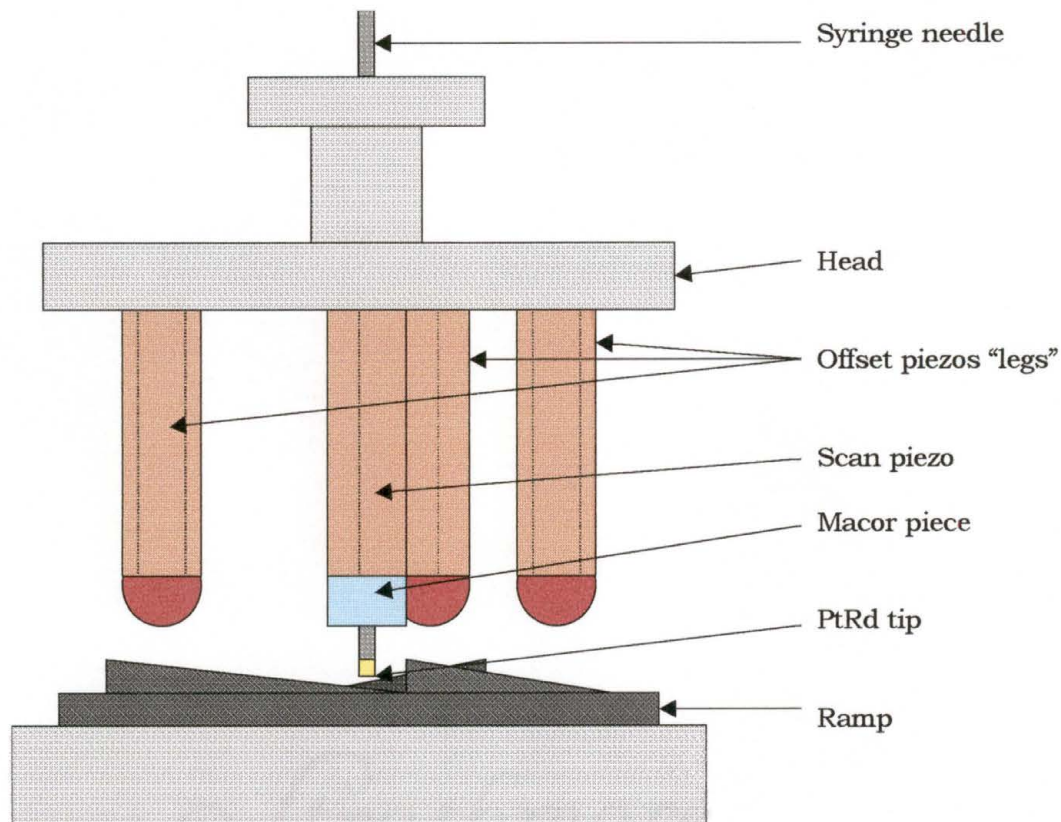


Figure 5.1 Head assembly of the Johnny Walker microscope.

The tip piezo is then mounted against stainless steel head with holes to feed the wires through. These piezo tubes have a 0.100" circumferential band on the end that connects to the stainless steel head; this eliminates grounding of the piezo. The tripod legs are attached to the head in a similar manner as the tip piezo.

A wire that is attached to the top plate of the vibration isolation stage applies the bias to the sample. The sample is set on this plate and silver pasted around its edges to ensure good electrical contact. The vibration isolation stage for the Johnny Walker assembly consists of four aluminum plates with cross sections of an o-ring in between them.

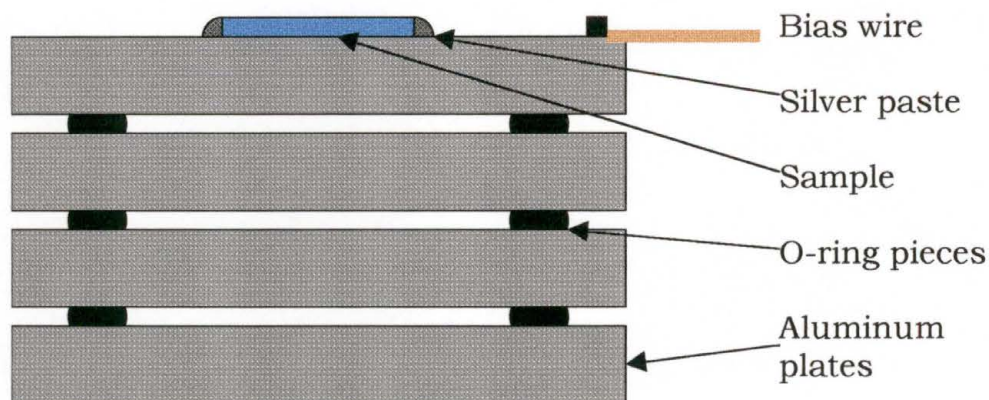


Figure 5.2 Vibration isolation stage for the JW model.

All the wires are attached to BNC connectors on the Faraday cage. BNC cables are then used to connect the cage to the rotary switch and the RHK control electronics.

5.1.2 MANIPULATOR

The manipulator is the apparatus used to raise and lower the head assembly onto the ramp assembly. It is completely detachable to eliminate the possibility of contributing mechanical noise to the head assembly.

5.1.3 WIRING

The wiring of the Johnny Walker was first done using 0.004" diameter wire. However, the lack of flexibility due to the larger diameter wire proved to be enough to hold the head assembly in place despite the efforts of its legs (3 offset piezos) to move it. Later, the Johnny Walker was fitted with 0.001" diameter wire to eliminate this problem.

5.1.4 FARADAY CAGE

The Faraday cage is made of a cubic aluminum frame with plexiglass sides and doors. To eliminate electromagnetic radiation through the plexiglass, a copper mesh was glued to the insides of the plexiglass. The plexiglass with the copper mesh on the inside is bolted to the frame to ensure contact between the frame and the copper mesh.

5.1.5 ROTARY SWITCH

A rotary switch controls this movement of the head assembly. The rotary switch is connected between the cage assembly and the RHK electronics. This rotary switch has 7 movement positions and an OFF position. Of the 7 movement positions, there is clockwise, counter clockwise, -x, +x, -y, +y, and offset. The clockwise and counter clockwise rotations are used to approach and retract from the sample. The -x, +x, -y, and +y positions are used to position the head assembly over desired sections of the sample.

Position	Direction
A	+X
B	+Y
C	Rotation-CW
D	Offset
E	-X
F	-Y
G	Rotation-CCW
H	OFF

Table 5.1 Switch positions and motion for Johnny Walker.

5.2 RHK STM-100 REV. 3 CONFIGURATION

For the Johnny Walker design, the RHK STM-100 REV. 3 control electronics is configured so that:

- a) the Z offset is not fed through the inertial input, redirects inertial input to X offset
- b) the Z offset is added Z signal
- c) the Z signal is added to X-Y scan piezos
- d) the Z offset is added to X-Y offset signals

See Appendix A for switch positions.

5.3 SPM 32 SOFTWARE CONFIGURATION

Again, the SPM 32 software allows the user to create a profile for an individual microscope so that the user does not have to adjust the parameters that differ between several microscopes. Examples on parameters that the profile contains are the scan head type, x, y, and z motion per piezo volt, and x, y, and z offset per piezo volt. See Appendix C for the parameter file for the Johnny Walker design.

5.4 SAMPLE APPROACH

After the manipulator has set the head assembly down onto the ramp, the tripod legs are utilized to approach the sample. Movement of the head assembly is achieved by using the stick-slip method discussed in previous chapters. The only difference is that the tubes are vertical, so that the slipping occurs between the balls and the ramp. The ramp is divided up into three 120-degree ramps, each of which one of the legs

rides on. This configuration allows for movement in the x and y direction and also rotation up and down the ramps. Movement in the x and y direction is primarily used for changing the image location on the sample. The clockwise rotation of the head assembly is used for approaching the sample until a tunneling current is produced. The counter clockwise rotation is used for retracting before moving to another image location or using the manipulator to move the head assembly.

5.5 FREQUENCY OF VIBRATION

The vibrations of the head assembly can be calculated to give an estimate of what resonance frequencies to expect under operation. We assume that the legs are attached to the ramp to simplify the calculation. We call the mass of the head (M) and the spring constant (K) of the three piezos. The spring constant (K) must be broken down into K_{\perp} for bending motions and K_{\parallel} for stretching motions. The equations for the spring constants are $K_{\perp} = \frac{3\pi}{64} E \frac{D^4 - d^4}{L^3}$ and $K_{\parallel} = \frac{\pi}{4} E \frac{D^2 - d^2}{L}$, where D is the outer diameter, d is the inner diameter, L is the length, and E is the elastic modulus of the piezo. [16]

The horizontal resonant frequency is found using $f_H = \frac{1}{2\pi} \sqrt{\frac{3K_{\perp}}{M}}$; the factor 3 is the number of piezos. The rotational resonant frequency is similar to the horizontal, but M and K_{\perp} are different. M and K_{\perp} are replaced with the moment of inertia $\frac{1}{2}(Mr^2)$ and the torsional spring

constant $K_{\perp}r^2$, where r is the distance of the tube from the center of the

head assembly. This results in $f_R = \frac{1}{2\pi} \sqrt{\frac{6K_{\perp}}{M}}$ being the rotational

resonant frequency. The vertical motion resonant frequency is found

using $f_V = \frac{1}{2\pi} \sqrt{\frac{3K_{\parallel}}{M}}$.

The dimensions of the piezo tubes for the Johnny Walker microscope are $L=10.16\text{mm}$, $D=3.175\text{mm}$, and $d=2.667\text{mm}$. The elastic modulus of the piezo tubes is $E=6.1 \times 10^{10} \text{ N/m}^2$. The calculated values of the spring constants are $4.37 \times 10^5 \text{ N/m}$ for bending motions (K_{\perp}) and $1.40 \times 10^7 \text{ N/m}$ for stretching motions (K_{\parallel}). The weight of the disk is approximately $4.0 \times 10^{-3} \text{ kg}$. The resulting calculated frequencies are listed in Table 5.2.

Horizontal resonance frequency	f_H	2.9kHz
Rotational resonance frequency	f_R	4.1kHz
Vertical resonance frequency	f_V	31.8kHz

Table 5.2 Resonance frequencies of the Johnny Walker design.

These are only estimations of noise frequencies to be aware of when imaging.

CHAPTER 6

EXAMPLES OF EXPERIMENTAL ANALYSIS IN STM

6.1 INSTRUMENTATION

Image analysis is the most important step of image production. An image in a readable format can make the understanding of data much clearer to the reader. Line Scans, 2-D Fast Fourier transforms, Angle Plots, Power Noise Spectrums, and 3-D Rotations of the image are all examples of image display options of the SPM-32 software. The raw data collected by the scanning tunneling microscopes can be corrected for hardware and alignment errors or clarified for ease of reading. Further image enhancement can be performed using graphical software such as Adobe PhotoShop, Microsoft Photo Editor, or Microsoft Image Composer. Care must be taken that vital information is not obscured or hidden by this processing.

6.2 FAST FOURIER TRANSFORMS

The Power Noise Spectrum menu of the SPM32 software generates a Fast Fourier transform of an input signal. The Fast Fourier transform measures the current per root frequency across a frequency range. By examining a null signal, these noise scans enable us to find

what frequency noises are affecting our imaging capabilities. Johnson noise or “white noise”, which is present in all resistors even when not in use, has a flat frequency spectrum. Flat frequency spectrum means that there is the same noise power in each hertz of frequency. The rms current ($I_{noise} (rms)$) per square root frequency bandwidth (B) is found using the equation

$$\frac{I_{noise} (rms)}{\sqrt{B}} = \left(\frac{4kT}{R}\right)^{\frac{1}{2}},$$

where k is Boltzmann’s constant, T is the temperature in Kelvin, and R is the resistance. At room temperature, the rms current per square root bandwidth is given by $1.27 \times 10^{-10} R^{-1/2}$. The preamplifier used in the tip circuitry has a $1 M\Omega$ resistor inside, so the rms current per square root bandwidth is $0.127 \frac{pA}{\sqrt{Hz}}$. As seen in Fig. 6.1 and Fig. 6.2, the noise is

less than 1 order of magnitude more than the theoretical limit.

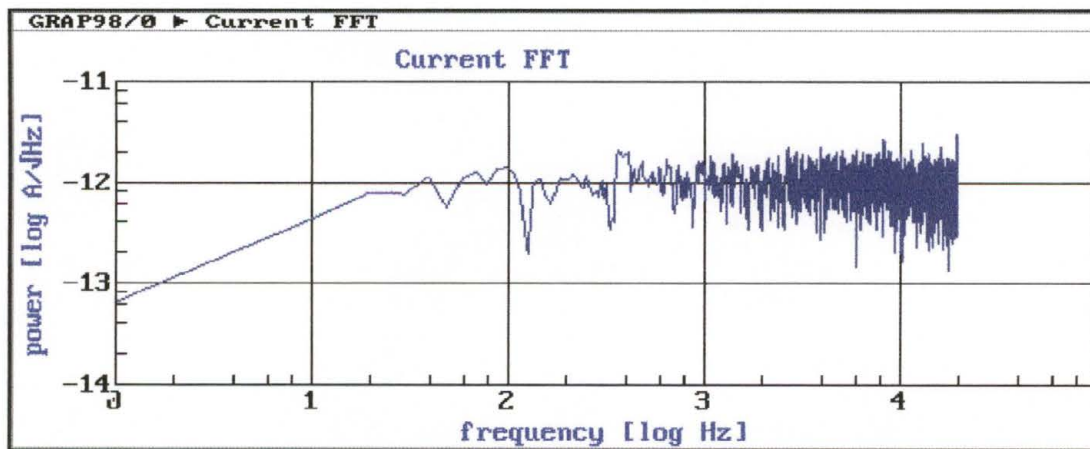


Figure 6.1 Fast Fourier transform of noise imaging while in tunneling range of the sample.

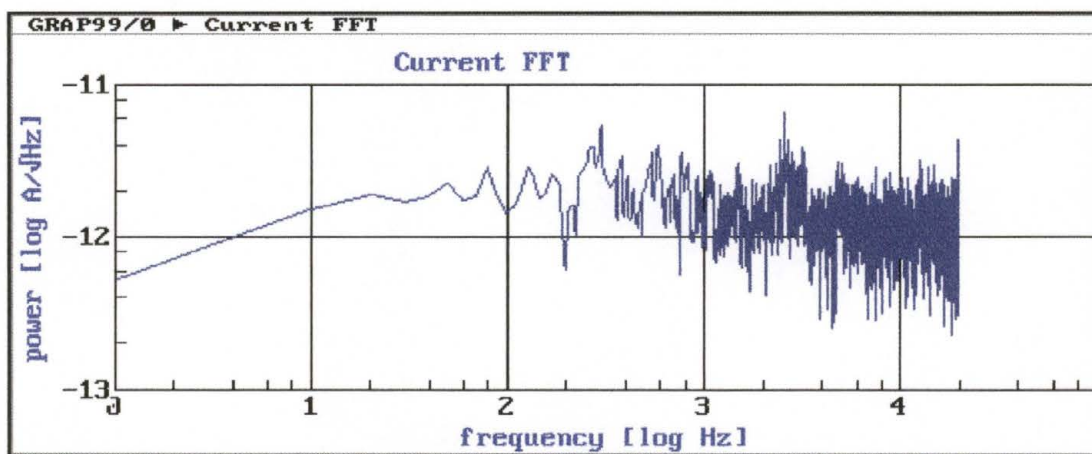


Figure 6.2 Fast Fourier transform of noise imaging while out of tunneling range of the sample.

6.3 EXAMPLES OF GRAPHITE DATA

Graphite has a hexagonal ($6 \times 60^\circ$) structure and its image is a 3-fold symmetric structure. Only the places that have atoms in the first and second layer are seen in an image scan, due to their higher current densities, than the just the surface atoms. The atoms that are imaged have an atomic spacing of 2.46 \AA , as seen in Fig. 6.3.

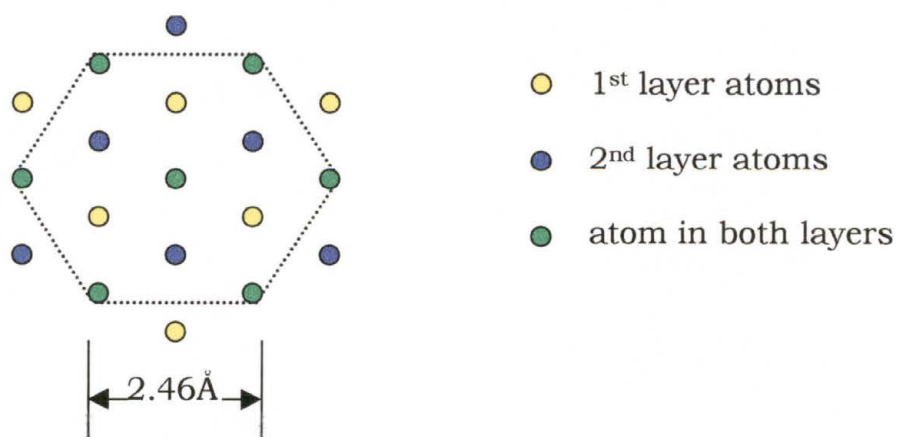


Figure 6.3 Atomic placement in hexagonal graphite structure.

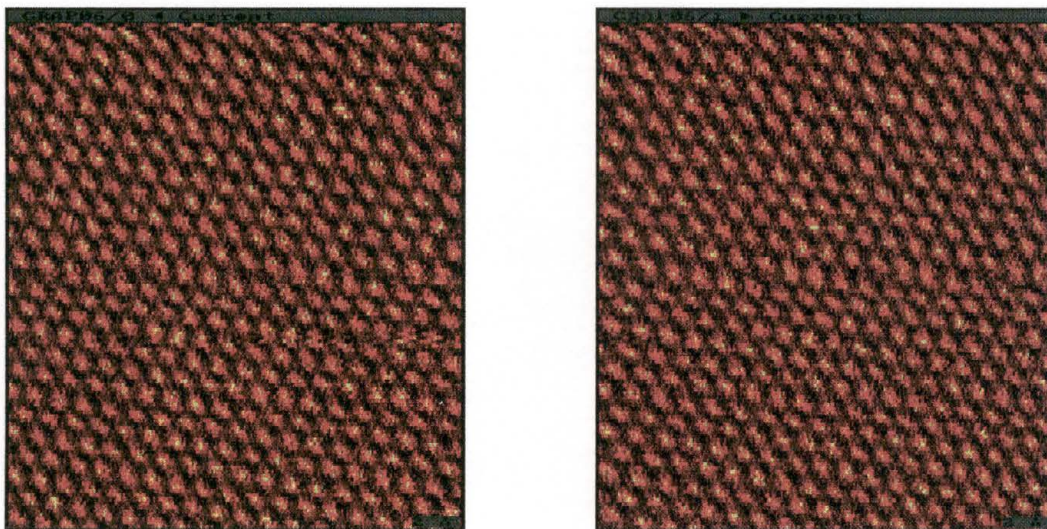


Figure 6.4 Raw graphite images taken simultaneously with the double tube design, one in the +x direction and the other in the -x direction.

An image can be clarified by subtracting the x offset, due to excessive swinging of the scan piezo. Also, smoothing the image eliminates erratic data, as seen in Fig 6.5.

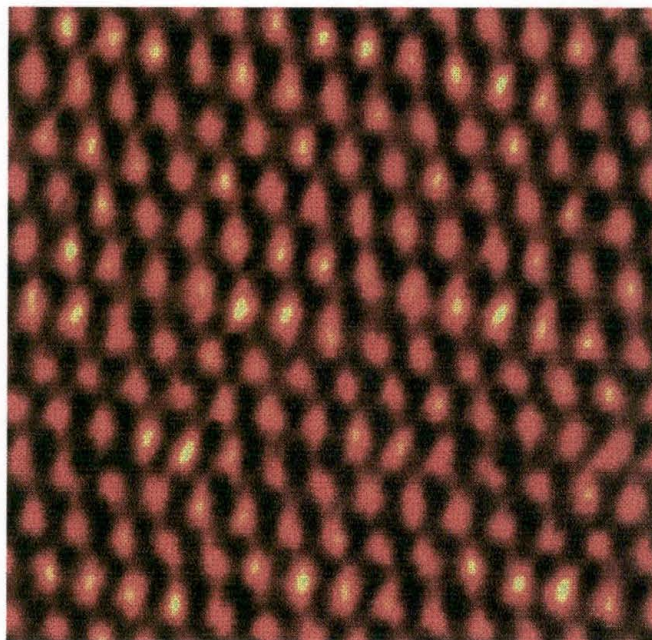


Figure 6.5 Graphite image after image enhancement.

A method of image correction is to perform a 2-D Fast Fourier transform. Performing a 2-D Fast Fourier transform on a graphite image produces an image of the repeating structure of the sample, seen in Fig. 6.6. To correct the shape of the structure, the SPM-32 allows the measurement and correction of the atomic spacing and the angle of the structure. The magnitude of the corrections can be used to calibrate the x and y scan motion per piezo volt.

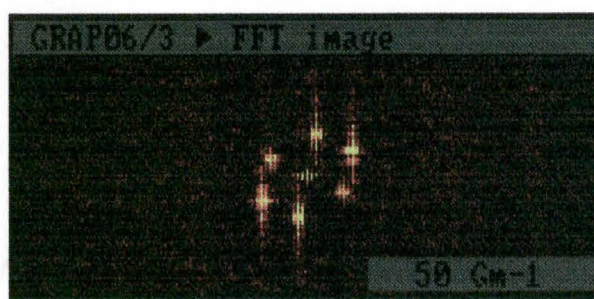


Figure 6.6 Fast Fourier transform performed on a graphite image.

In Fig. 6.7, a line scan taken from an image gives a cross-sectional view of the sample. With this view of the sample, it is easier to analyze the features and see the atomic spacing of the graphite sample.

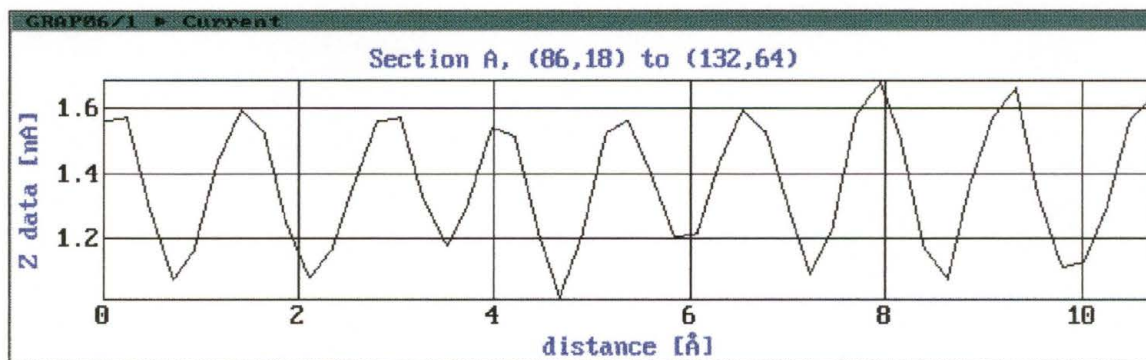


Figure 6.7 Line scan across a graphite sample.

6.4 EXAMPLES OF METALLIC SAMPLE

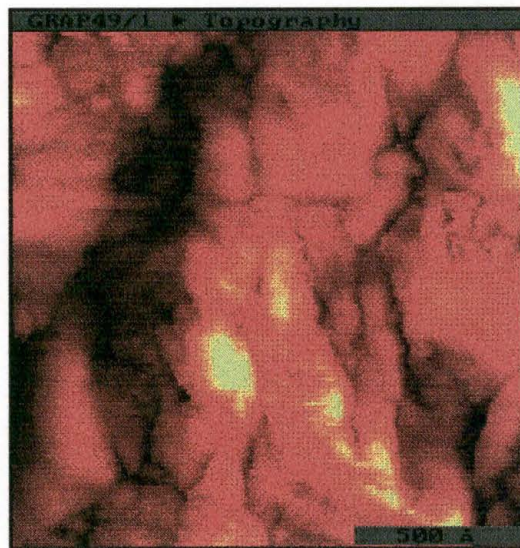


Figure 6.8 Raw silver image taken with the double tube design.

A line scan produces a side view of the sample without having to cleave the sample.

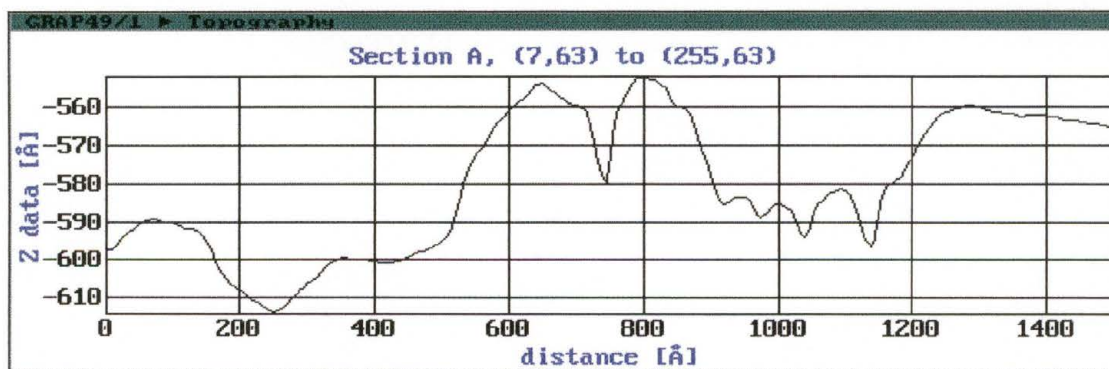


Figure 6.9 Line scan across a silver sample.

A 3-D rotational plot of a silver sample sputtered on a DC Magnetron system. This plot allows the reader to visually see the grain boundaries across the silver sample.

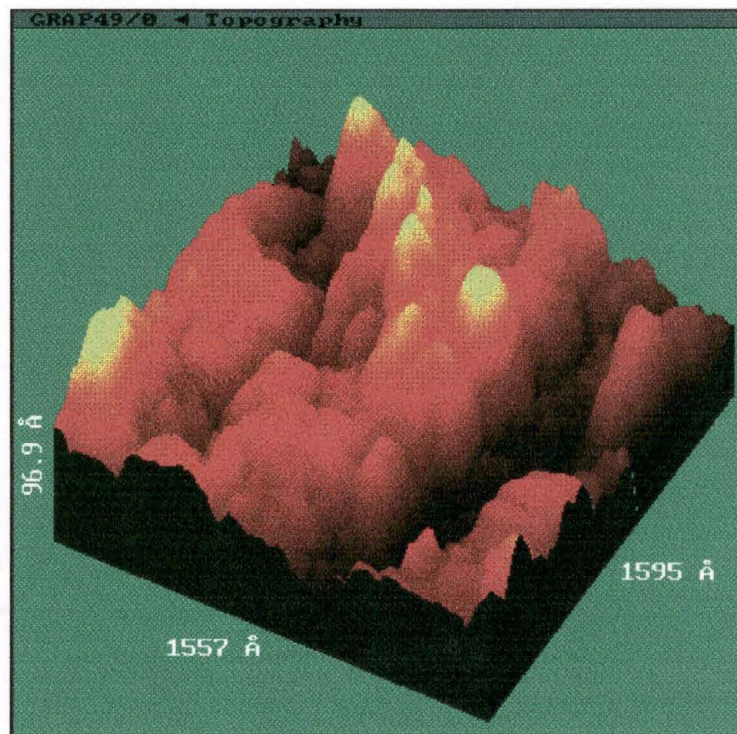


Figure 6.10 A 3-D rotated image of a silver sample.

CHAPTER 7

ELECTROCHEMICAL SCANNING TUNNELING MICROSCOPY

Electrochemical Scanning Tunneling Microscopy (ESTM) was designed to enable imaging a sample that is submersed in electrolytic solution. In other words, to image a sample while an electrochemical reaction occurred. An ESTM approaches and scans the tip across the surface of the sample the same way an STM does. Also, the tunneling current is recorded in the same manner as before. However, some modifications and additions must be made to an STM to perform image samples in an electrolytic solution. An electrochemical reaction causes a change in the surface structure of the sample. The difference between images reflect the alteration in composition and structure of the sample. ESTM has numerous abilities, such as the study of metal deposition, surface anodization, nanolithography, and atomic manipulation. [2-9]

7.1 THEORY

Electrochemistry deals with both the chemical and the electrostatic properties of free charged particles. Electrical currents in conductors are the directed motions of free charge under the influence of an applied

electric field. The conduction can be electronic, ionic, or both, depending on the kind of charge involved. Electronic conduction is found in all metals and also in certain other substances: carbon materials (graphite, carbon black), some oxides and other inorganic compounds (tungsten carbide), and a number of organic substances. Ionic conduction is found in a broad selection of substances known as electrolytes or conductors of the second kind. Electrolytes can be distinguished into different groups, for example, aqueous solutions of salts, acids, bases and salt melts.

The tunneling of electrons in an aqueous solution is much more complicated than tunneling through a vacuum or the ambient air. Submersing the sample in a solution increases the difficulty due to the possibility of background current through the solution. Background currents are very likely in an electrolytic solution. Some additional scattering may also affect the tunneling process. The background current should only have a weak dependence of the tip-sample distance compared to the tunneling current allowing the imaging process to continue to work.

7.2 ELECTROCHEMICAL CELL

An electrochemical cell has many working parts such as the bipotentiostat, counter electrode, working electrode, reference electrode, and the cell material and volume. The bipotentiostat used here at SWTSU is an AFCBP1 Bipotentiostat from Pine Instrument Company.

The counter electrode (CE) of the cell should be relatively large and axially symmetric with respect to the working electrode (WE). This electrode geometry ensures a uniform electric field through the cell and should have a submerged area of approximately 100mm^2 . The counter electrode should be made of the same material as the WE. The reference electrode (RE) is positioned as close to the WE as possible, to minimize ohmic losses, and thus allow the potential difference between the two electrodes to be readily controlled. The working electrode is applied to the sample with a submerged area of approximately 10mm^2 .

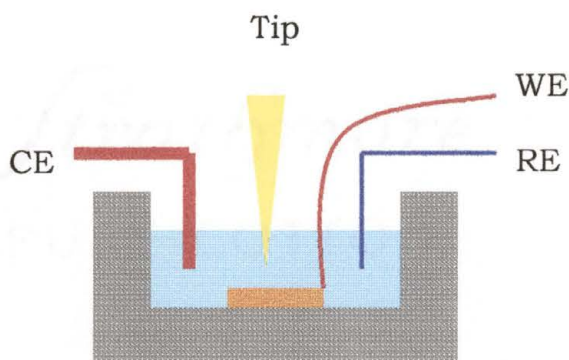


Figure 7.1 Two-dimensional side view of an electrochemical cell.

Electrochemical cells must be made from materials that are chemically inert, free of surface-active agents, and easily cleaned. Two materials that have these qualities are Teflon™ and KEL-F plastic™. The first cell was made from Teflon™ due to cost, to make alterations affordable if they are necessary. The final cell will be made from KEL-F plastic™, because of its greater dimensional stability than Teflon™. Design considerations were taken from current developments in scientific

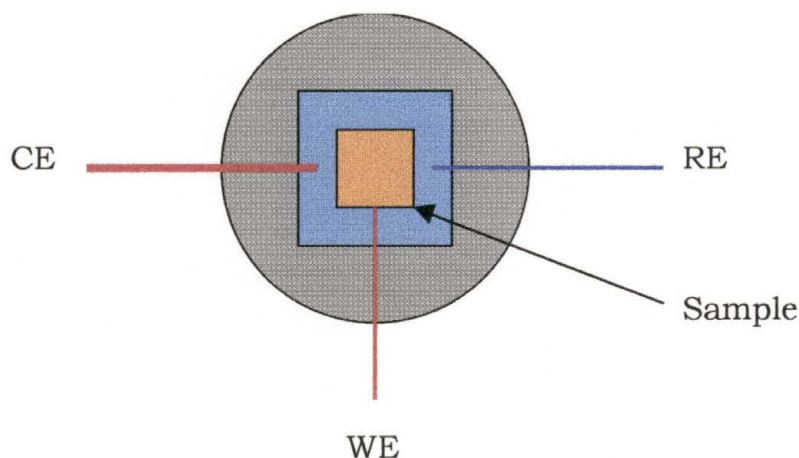


Figure 7.2 Two-dimensional top view of an electrochemical cell.

literature. A major design consideration of an electrochemical cell is the size of the samples that will be imaged. With different volumes and different shapes, careful testing must be done to establish acceptable electrode locations and solution fill levels in the cell. For example, a total cell volume of approximately 0.46 ml is filled with approximately 0.2 ml of the electrolytic solution. Examples of electrolytic solutions are doubly distilled water, water and H_2SO_4 , and Na_2SO_4 and CuSO_4 . [16] The tip is insulated with Apiezon wax or nail polish to minimize Faradic background.

The cell will then be mounted on the Johnny Walker microscope and the sample ground will be attached (cell is made of an insulating material so grounding will be a problem), see Fig. 7.3 for location of the cell. The bipotentiostat will then be added to the system to control reactions at the surface of the sample while the STM measures changes in topography.

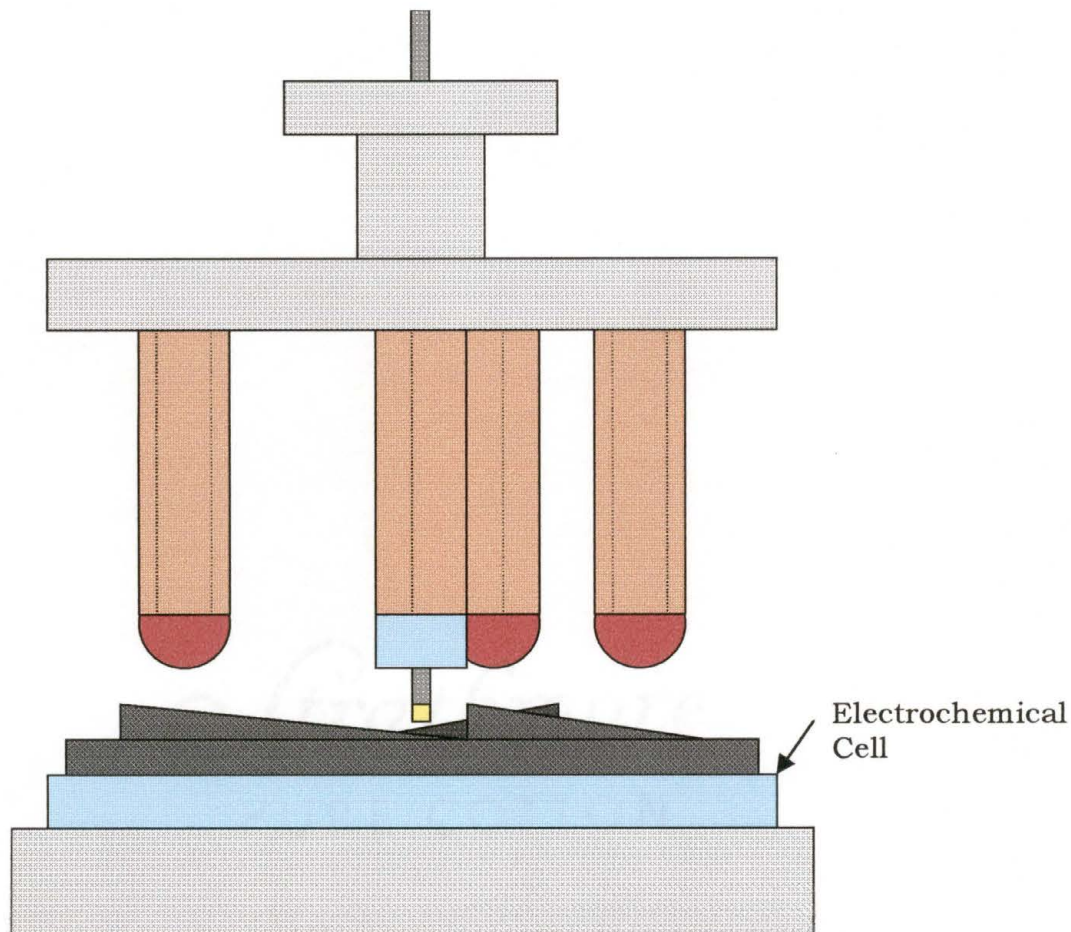


Figure 7.3 Johnny Walker microscope with the addition of the electrochemical cell.

7.3 APPLICATIONS/RESEARCH AREAS

An electrochemical cell provides an atmosphere where the surface cleanliness and preparation can be controlled reliably and where industrial situations can be simulated. Possible systems to study are the chemical mechanical polishing (CMP) of silicon wafers with partially completed devices. Chemical mechanical polishing in wafer production

is used for planarization of tungsten and oxide surfaces and is important element of producing circuits with copper interconnects. ESTM can be useful in determining and predicting characteristics of the CMP process, such as reaction rates, the influence of surface structure, and grain boundaries. Surface modification of the sample using ESTM such as, metal deposition on GaAs or surface anodization to locally oxidize a silicon substrate are additional possibilities. In ESTM, the tip can be used to direct the deposition of a molecule in the solution or to cause an oxide to grow underneath the tip's path.

CHAPTER 8

CONCLUSIONS

8.1 STM AND ELECTROCHEMISTRY

Scanning Tunneling Microscopy has proven to be a crucial tool for the determination of the structural and electrical properties of surfaces. Today, STM experiments can be performed in a variety of environments: air, inert gas, ultrahigh vacuum, or even liquids. Many related techniques have been developed since the creation of STM, such as, local spectroscopy, scanning potentiometry and other local probes. The desire to build an STM that images in liquids, fueled the need for a vertical style microscope, i.e. Johnny Walker. Since, Johnny Walker has a tripod configuration for sample approaches, the need for a multifunctional switch was necessary for motion of the head assembly. Also since liquids are conductors, a non-conductive cell manufactured to the necessary dimensions to act as Johnny Walker's sample holder. The addition of electrochemistry to STM has created even more techniques such as metal deposition, surface anodization, electrochemical nanolithography, and atomic manipulation. [2-9]

8.2 FUTURE CONSIDERATIONS

Possible future systems to study here at SWTSU are solution-sample reactions, the chemical mechanical polishing of silicon wafers with partially completed devices, metal deposition on GaAs, and surface anodization to locally oxidize a silicon substrate. [2-5] Other possible research areas are surface techniques such as the creation of holes by voltage pulses, creation of lines by scanning with a large tunneling current, or even atomic manipulation. [2-9]

APPENDIX

Appendix A

RHK MODEL STM 100 SWITCH POSITION OPTIONS

Board 1

Sw1: Position 1-2: does not allow Z-offset from inertial input, redirects inertial input to X offset

Position 2-3: feeds Z-offset through inertial input

Board 6

Sw1: Position 1-2: feeds X from rear panel BNC through X-Y interface board (6)

Position 2-3: feeds X from scan generator board (7) through X-Y interface board (6)

Sw2: Position 1-2: feeds Y from rear panel BNC through X-Y interface board (6)

Position 2-3: feeds Y from scan generator board (7) through X-Y interface board (6)

Sw3: Position 1-2: input from Z offset board, Z offset knobs control voltage at Z offset output

Position 2-3: output to Z driver board, Z offset is added to Z signal

Board 9

Sw1: Position 1-2: adds Z signal to X-Y scan piezos, should be nothing connected to Z signal

Position 2-3: doesn't add Z signal to X-Y scans, use if you have Z signal connected

Sw2: Position 1-2: X scan knob controls X scan range at X scan piezos

Position 2-3: use for external control of X scan

Sw3: Position 1-2: Y scan knob controls Y scan range at Y scan piezos

Position 2-3: use for external control of Y scan

Board 10

Sw1: Position 1-2: adds Z offset to X-Y offset signals, use if nothing connected to Z offset

Position 2-3: doesn't add Z offset to X-Y offset signals, use if Z offset is connected

Sw2: Position 1-2: X offset knob controls X offset,

Position 2-3: X offset externally controlled

Sw3: Position 1-2: Y offset knob controls Y offset

Position 2-3: Y offset externally controlled

The switch positions for Johnny Walker are:

Board 1: sw1: 1-2

Board 6: sw1: 2-3, sw2: 2-3, sw3: 2-3

Board 9: sw1: 1-2, sw2: 1-2, sw3: 1-2

Board 10: sw1: 1-2, sw2: 1-2, sw3: 1-2

The switch positions for Double Tube are:

Board 1: sw1: 2-3

Board 6: sw1: 2-3, sw2: 2-3, sw3: 1-2

Board 9: sw1: 2-3, sw2: 1-2, sw3: 1-2

Board 10: sw1: 2-3, sw2: 1-2, sw3: 1-2

Appendix B**SPM 32 DOUBLE TUBE CONFIGURATION FILE**

Scan Head Parameters

11,01;Head type, approach: 2, 0

11,02;Double tube

11,03;scan: 3.89e-09, 5.801e-09, 1.5e-09

11,04;offset: 2.5e-09, 2.5e-09, 3.024e-09

Electronics Parameters

12,01;Electronics type: 1, 1, 0, 1

Monitor calibrations:

12,03;scan: 13.000000, 13.000000, 13.000000

12,04;offset: 13.000000, 13.000000, 13.000000

12,05;preamp: 1e-08, 1

12,06;scan zero: 0, 0

Interface Parameters

13,01;DT-2821 Base address, type: 240, 1, 300000, 1000

13,03;TTL: 228, 0

13,04;Counter: 1A0, 0

13,05;MCA: 292, 0

Acquisition Parameters

14,01;signal: 0

14,02;lbl gain and speed: 0, 7

14,03;Aux

14,04;V

14,05;aux gain: 1, 1, 0.5, 0, 1, 1

14,08;noise source, gain, rate, loop, points, sum, average: 1, 0, 8, 0, 2, 0,
2, 0, 0
14,13;User
14,14;V
14,15;IV control: 1, 1, 5, 0, 1, 1, 1, 0, 0, 0, 0, 0, 1, 2
14,16;IV range: -1, 1, 0.04883, 0, 0, 1e-07, 1
14,17;IV time: 0.01, 0.05, 1, 5e-11, 1e-09, 1e-10, 0
14,18;IZ control: 1, 2, 5, 0, 1, 1, 1, 0, 0, 0, 0, 0, 1, 2
14,19;IZ range: 1e-09, -1e-09, 4.883e-11
14,20;IZ time: 0.01, 0.05, 1e-09
14,21;Save status: 0.1, 0, 0, 0, 0, 0, 0
14,22;Slider: 1
14,23;Multivolt: 0, 2, 1, -1, 1, -1, 0.001, 1
14,24;Scan display: 1, 0, 0
14,25;Lithography: 1, 1, 0, 1, 5, 0.001, 0.0005
14,26;scan delay: 0, 0, 0
14,27;image out: 0, 2, 0, 4, 1, 0, 0.01, 0, 0
14,28;Aux 1
14,29;V
14,30;Aux 2
14,31;V
14,32;Stepper: 1, 1, 1, 0, 0.02
14,33;Phi UHV: 1, 0.0005, 0.0005, 0.01
14,34;A1 rate
14,35;Hz
14,37;Counter: 0, 0.01, 1, 1
14,38;A2 rate
14,39;Hz
14,40;image modes: 0, 0, 0, 0, 0, 0
14,41;image channels: 0, 1, 0, 0, 0, 0, 0
14,42;image gains: 0, 0, 0, 0, 0, 0, 0

14,43;inchworm: 0.0001, 5e-05, 6.7e-09, 0, 0, 0, 1e-05
14,44;approach: 0, 1, 1, 1, -100, 1e-09, 1, 0.5, 0.5, 10, 0.01, 0
14,45;waveform: 0, 1, 0, 0.001, -1e-07, 0, 1
14,46;MCA: 0, 10, 0.1, 1, 1, 1, 1
14,47;MCA Data
14,48;V
14,49;Hz
14,50;waveform: 2e-06, 2e-06, 5e-07, 4e-07, 1e-07
14,51;newscope: -6, 6, 1, 3
14,52;scope1: 0, -29, 0, 1, 0
14,53;scope2: 1, 0, 0, 4, 0
14,54;scope3: 2, 0, 0, 2, 0
14,55;scope4: 1, 0, 0, 15, 0
14,56;AFM: 0.01, 0.00015, 10, 50, 0, 1, 0.5
14,57;AFM2: 1, 0, 0, 1, 1
14,58;Force gradient
14,59;N/m
14,60;Multigap: 1e+08, 1e+08, 1e+08, 1e+08
14,61;newline: -28, 0, 1, 8
14,62;line1: 0, -31, 2, 14, 0
14,63;line2: 1, 0, 0, 4, 0
14,64;line3: 2, 0, 0, 2, 0
14,65;line4: 1, 0, 0, 15, 0
14,66;scope color2: 15, 12, 10, 7, 9, 12, 10, 7
14,67;imageline: -24, 0, 1, 8
14,68;image1: 3, -7, 0, 1, 0
14,69;image2: 1, 0, 0, 4, 0
14,70;image3: 2, 0, 0, 2, 0
14,71;image4: 1, 0, 0, 15, 0

Disk I/O Parameters

16,01;C:
16,02;\SPM\NOWSPM32\TESTING\
16,03;auto_name: 1, 1, 0
16,04;DTINA
16,05;40
16,06;GRAP
16,07;02
16,08;
16,09;SM2
16,10;SM2

Plot and Display Options

17,01;Resolution, limit, dump: 2, 40, 1, 1, 0
17,02;Colortable, contrast, steps: 1
17,04;Interface click, screen, input, error delay, mouse, psc: 0.35, 500,
1.50, 0.00, 0, 0, 0, 1, 1, 0, 1, 50, 5
17,05;Map defaults, size, theta, phi, mode: 2, 30, 15
17,06;Chart defaults, size, scale, skip: 2, 1.000, 1
17,07;3-D defaults, size, angles, mode, fill, scale, skip: 3, 30, 20, 1, 3, 5
17,08;Color values: 29, 63, 22, 0
17,08;Color values: 40, 63, 63, 0
17,08;Color values: 41, 0, 45, 40
17,08;Color values: 42, 63, 63, 63
17,08;Color values: 43, 0, 0, 0
17,08;Color values: 31, 0, 32, 32
17,08;Color values: 32, 0, 0, 0
17,08;Color values: 19, 48, 35, 20
17,08;Color values: 18, 0, 0, 0
17,08;Color values: 20, 60, 60, 60
17,08;Color values: 21, 0, 50, 50
17,08;Color values: 24, 0, 0, 45

17,08;Color values: 35, 47, 47, 47

17,08;Color values: 36, 0, 0, 0

17,08;Color values: 33, 0, 14, 17

17,08;Color values: 34, 0, 63, 47

17,08;Color values: 38, 0, 0, 0

17,08;Color values: 39, 0, 63, 63

17,09;Interface pop, new, change save: 0, 1, 0, 1, 0, 1, 2, 0

17,10;Tag defaults: 0, 0, 0, 0

17,11;Graph defaults: 2 1 1 8

17,12;Window values: 1, 0, 551, 217, 248, 272

17,12;Window values: 2, 0, 696, 640, 328, 128

17,12;Window values: 3, 0, 488, 478, 248, 272

17,12;Window values: 4, 0, 396, 634, 224, 112

17,12;Window values: 5, 0, 748, 512, 232, 256

17,12;Window values: 6, 0, 87, 303, 264, 208

17,12;Window values: 7, 1, 659, 257, 328, 224

17,12;Window values: 8, 1, 682, 46, 296, 192

17,12;Window values: 9, 0, 752, 32, 272, 336

17,12;Window values: 10, 0, 0, 302, 264, 256

17,12;Window values: 11, 0, 736, 32, 272, 256

17,12;Window values: 12, 0, 462, 560, 248, 208

17,12;Window values: 13, 0, 420, 357, 240, 96

17,12;Window values: 14, 0, 427, 412, 240, 240

17,12;Window values: 15, 0, 526, 487, 168, 144

17,12;Window values: 16, 0, 751, 478, 232, 272

17,12;Window values: 18, 0, 230, 606, 248, 160

17,12;Window values: 19, 0, 841, 447, 168, 80

17,12;Window values: 20, 0, 6, 308, 605, 180

17,12;Window values: 21, 0, 748, 368, 264, 400

17,12;Window values: 22, 0, 750, 464, 256, 304

17,12;Window values: 23, 0, 516, 523, 256, 144

17,12;Window values: 24, 0, 748, 300, 256, 256
17,12;Window values: 25, 1, 359, 343, 272, 144
17,12;Window values: 26, 0, 317, 377, 192, 96
17,12;Window values: 27, 0, 743, 544, 240, 224
17,12;Window values: 29, 0, 100, 100, 160, 265
17,12;Window values: 30, 1, 529, 32, 20, 256
17,12;Window values: 33, 1, 5, 33, 260, 270
17,12;Window values: 34, 1, 276, 32, 260, 270
17,12;Window values: 38, 0, 109, 350, 208, 224
17,12;Window values: 39, 1, 676, 296, 328, 176
17,12;Window values: 41, 1, 12, 489, 965, 260
17,12;Window values: 45, 0, 584, 495, 240, 160
17,12;Window values: 46, 0, 739, 608, 224, 160
17,12;Window values: 47, 0, 472, 496, 232, 176
17,12;Window values: 51, 0, 741, 432, 264, 336
17,12;Window values: 52, 0, 131, 588, 725, 180
17,12;Window values: 53, 0, 752, 544, 272, 224
17,12;Window values: 54, 0, 744, 576, 256, 192
17,12;Window values: 56, 1, 0, 402, 280, 320
17,12;Window values: 57, 0, 244, 704, 144, 32
17,12;Window values: 58, 0, 751, 592, 256, 176
17,12;Window values: 59, 1, 426, 562, 400, 32
17,12;Window values: 60, 0, 128, 400, 512, 80
17,12;Window values: 61, 0, 568, 81, 160, 240
17,14;Graph colors: 15 1 2 3 4 0 0 0
17,15;version: 4
17,16;print
17,17;C:
17,18; \SPM\NOWSPM32\ADVLAB\WANDT\
17,19;OUT
17,20;68C

17,22;Contrast modes: 0, 1, 1, 0, 2, 0
17,23;Contrast: 1e-06, -1e-06, 0, 1
17,24;Transform: 0, 1, 0, 1, 1, 1
17,25;Tutor: 581

Process Options

18,01;Fourier mode: 3, 2
18,02;Fourier levels: 1e-08, 0.001, 0.5, 2
18,03;Fourier notch: 0, 0, 1, 1
18,04;Fourier notch freq: 1e+09, 1e+09, 1e-11, 0
18,05;Autocorrelate: 50, 0, 0, 0, 0, 0, 1, 1
18,06;
18,07;
18,08;

DSP stuff

19,08;DSP control: 290, 0, 0, 1, 1, 3, 3
19,09;c:\stm386\a.out
19,10;DSP offset: 0, 0, 0, 1e-06
19,11;DSP loop: 0.1, 1e-09, 1e-06, 100
19,12;DSP scan1: 1e-07, 1e-07, 0, 0, 1e-06, 0
19,13;DSP scan2: 0, 0, 0, 0, 1
19,14;DSP head: 5e-09, 5e-09, 1.5e-09, 0, 0, 0
19,15;DSP gain1: 1, 1, 1, 1, 1, 1
19,16;DSP gain2: 1, 1, 1e-09, 0
19,17;DSP jerk1: 1e-07, 1e-07, 0.0001, 0.01, 1e-09, 30
19,18;DSP jerk2: 50, 50, 1, 1, 0
19,19;DSP knob: 0, 0, 0, 0, 0, 0, 0, 0
19,20;DSP move: 0.5, 0.2, 5e-10, 1e-09, 0, 0.001, 1e-07

Appendix C**SPM 32 JOHNNY WALKER CONFIGURATION FILE**

Scan Head Parameters

11,01;Head type, approach: 4, 0
11,02;Johnny Walker
11,03;scan: 3.89e-09, 5.801e-09, 1.5e-09
11,04;offset: 2.5e-09, 2.5e-09, 1.5e-09

Electronics Parameters

12,01;Electronics type: 1, 1, 0, 1
Monitor calibrations:
12,03;scan: 13.000000, 13.000000, 13.000000
12,04;offset: 13.000000, 13.000000, 13.000000
12,05;preamp: 1e-08, 1
12,06;scan zero: 0, 0

Interface Parameters

13,01;DT-2821 Base address, type: 240, 1, 300000, 1000
13,03;TTL: 228, 0
13,04;Counter: 1A0, 0
13,05;MCA: 292, 0

Acquisition Parameters

14,01;signal: 0
14,02;lbl gain and speed: 0, 7
14,03;Aux
14,04;V
14,05;aux gain: 1, 1, 0.5, 0, 1, 1

14,08;noise source, gain, rate, loop, points, sum, average: 0, 0, 4, 0, 2, 0, 2, 0, 0
14,13;User
14,14;V
14,15;IV control: 1, 1, 5, 0, 1, 1, 1, 0, 0, 0, 0, 0, 1, 2
14,16;IV range: -1, 1, 0.04883, 0, 0, 1e-07, 1
14,17;IV time: 0.01, 0.05, 1, 5e-11, 1e-09, 1e-10, 0
14,18;IZ control: 1, 2, 5, 0, 1, 1, 1, 0, 0, 0, 0, 0, 1, 2
14,19;IZ range: 1e-09, -1e-09, 4.883e-11
14,20;IZ time: 0.01, 0.05, 1e-09
14,21;Save status: 0.1, 0, 0, 0, 0, 0, 0, 0
14,22;Slider: 1
14,23;Multivolt: 0, 2, 1, -1, 1, -1, 0.001, 1
14,24;Scan display: 1, 0, 0
14,25;Lithography: 1, 1, 0, 1, 5, 0.001, 0.0005
14,26;scan delay: 0, 0, 0
14,27;image out: 0, 2, 0, 4, 1, 0, 0.01, 0, 0
14,28;Aux 1
14,29;V
14,30;Aux 2
14,31;V
14,32;Stepper: 1, 1, 1, 0, 0.02
14,33;Phi UHV: 1, 0.0005, 0.0005, 0.01
14,34;A1 rate
14,35;Hz
14,37;Counter: 0, 0.01, 1, 1
14,38;A2 rate
14,39;Hz
14,40;image modes: 0, 0, 0, 0, 0, 0
14,41;image channels: 1, 0, 0, 0, 0, 0, 0
14,42;image gains: 0, 0, 0, 0, 0, 0, 0

14,43;inchworm: 0.0001, 5e-05, 6.7e-09, 0, 0, 0, 1e-05
14,44;approach: 0, 1, 1, 1, -100, 1e-09, 1, 0.5, 0.5, 10, 0.01, 0
14,45;waveform: 0, 1, 0, 0.001, -1e-07, 0, 1
14,46;MCA: 0, 10, 0.1, 1, 1, 1, 1
14,47;MCA Data
14,48;V
14,49;Hz
14,50;waveform: 1e-06, 1e-06, 1e-07, 1e-07, 1e-07
14,51;newscope: -6, 6, 1, 3
14,52;scope1: 0, -5, 0, 1, 0
14,53;scope2: 1, -5, 0, 4, 0
14,54;scope3: 2, -5, 0, 2, 0
14,55;scope4: 1, -5, 0, 15, 0
14,56;AFM: 0.01, 0.00015, 10, 50, 0, 1, 0.5
14,57;AFM2: 1, 0, 0, 1, 1
14,58;Force gradient
14,59;N/m
14,60;Multigap: 1e+08, 1e+08, 1e+08, 1e+08
14,61;newline: -24, 0, 1, 8
14,62;line1: 0, -31, 2, 14, 0
14,63;line2: 1, 0, 0, 4, 0
14,64;line3: 2, 0, 0, 2, 0
14,65;line4: 1, 0, 0, 15, 0
14,66;scope color2: 15, 12, 10, 7, 9, 12, 10, 7
14,67;imageline: -24, 0, 1, 8
14,68;image1: 3, -7, 0, 1, 0
14,69;image2: 1, 0, 0, 4, 0
14,70;image3: 2, 0, 0, 2, 0
14,71;image4: 1, 0, 0, 15, 0

Disk I/O Parameters

16,01;C:
16,02;\NOWSPM32\TESTINGJ\
16,03;auto_name: 1, 1, 0
16,04;DTINA
16,05;00
16,06;GRAP
16,07;28
16,08;
16,09;SM2
16,10;SM2

Plot and Display Options

17,01;Resolution, limit, dump: 2, 40, 1, 1, 0
17,02;Colortable, contrast, steps: 1
17,04;Interface click, screen, input, error delay, mouse, psc: 0.35, 500,
1.50, 0.00, 0, 0, 0, 1, 1, 0, 1, 50, 5
17,05;Map defaults, size, theta, phi, mode: 2, 30, 15
17,06;Chart defaults, size, scale, skip: 2, 1.000, 1
17,07;3-D defaults, size, angles, mode, fill, scale, skip: 3, 30, 20, 1, 3, 1
17,08;Color values: 29, 34, 31, 31
17,08;Color values: 40, 63, 63, 0
17,08;Color values: 41, 0, 0, 0
17,08;Color values: 42, 63, 63, 63
17,08;Color values: 43, 0, 0, 0
17,08;Color values: 31, 0, 32, 32
17,08;Color values: 32, 0, 0, 0
17,08;Color values: 19, 48, 35, 20
17,08;Color values: 18, 0, 0, 0
17,08;Color values: 20, 60, 60, 60
17,08;Color values: 21, 0, 50, 50
17,08;Color values: 24, 0, 0, 45

17,08;Color values: 35, 47, 47, 47

17,08;Color values: 36, 0, 0, 0

17,08;Color values: 33, 0, 14, 17

17,08;Color values: 34, 0, 63, 47

17,08;Color values: 38, 0, 0, 0

17,08;Color values: 39, 0, 63, 63

17,09;Interface pop, new, change save: 0, 1, 0, 1, 0, 1, 2, 0

17,10;Tag defaults: 0, 0, 0, 0

17,11;Graph defaults: 2 0 0 8

17,12;Window values: 1, 0, 551, 217, 248, 272

17,12;Window values: 2, 0, 696, 640, 328, 128

17,12;Window values: 3, 0, 746, 496, 248, 272

17,12;Window values: 4, 0, 396, 634, 224, 112

17,12;Window values: 5, 0, 748, 512, 232, 256

17,12;Window values: 6, 1, 760, 32, 264, 208

17,12;Window values: 7, 0, 696, 526, 328, 224

17,12;Window values: 8, 1, 0, 576, 312, 192

17,12;Window values: 9, 0, 409, 412, 272, 336

17,12;Window values: 10, 1, 1, 308, 272, 256

17,12;Window values: 11, 1, 752, 243, 272, 256

17,12;Window values: 12, 0, 462, 560, 248, 208

17,12;Window values: 14, 0, 427, 412, 240, 240

17,12;Window values: 16, 0, 299, 419, 224, 272

17,12;Window values: 18, 0, 123, 589, 240, 160

17,12;Window values: 21, 0, 748, 368, 264, 400

17,12;Window values: 22, 0, 750, 464, 256, 304

17,12;Window values: 23, 0, 539, 524, 264, 144

17,12;Window values: 24, 1, 760, 512, 256, 256

17,12;Window values: 25, 1, 409, 360, 272, 144

17,12;Window values: 26, 0, 317, 377, 192, 96

17,12;Window values: 27, 0, 743, 544, 240, 224

17,12;Window values: 30, 0, 529, 32, 20, 256
17,12;Window values: 33, 1, 0, 32, 260, 270
17,12;Window values: 34, 1, 263, 32, 260, 270
17,12;Window values: 38, 0, 109, 350, 208, 224
17,12;Window values: 39, 0, 329, 462, 312, 176
17,12;Window values: 41, 0, 4, 505, 965, 260
17,12;Window values: 45, 0, 584, 495, 240, 160
17,12;Window values: 46, 0, 739, 608, 224, 160
17,12;Window values: 47, 1, 527, 592, 232, 176
17,12;Window values: 51, 0, 741, 432, 264, 336
17,12;Window values: 52, 0, 131, 588, 725, 180
17,12;Window values: 53, 0, 752, 544, 272, 224
17,12;Window values: 54, 0, 744, 576, 256, 192
17,12;Window values: 56, 0, 501, 53, 280, 320
17,12;Window values: 57, 0, 244, 720, 200, 32
17,12;Window values: 58, 0, 751, 592, 256, 176
17,12;Window values: 59, 0, 312, 448, 384, 64
17,12;Window values: 60, 0, 144, 400, 240, 48
17,12;Window values: 61, 1, 346, 528, 160, 240
17,14;Graph colors: 15 1 2 3 4 0 0 0
17,15;version: 4
17,16;print
17,17;C:
17,18;\n
17,19;OUT
17,20;22
17,22;Contrast modes: 0, 1, 1, 0, 2, 0
17,23;Contrast: 1e-06, -1e-06, 0, 1
17,24;Transform: 0, 1, 0, 1, 1, 1
17,25;Tutor: 581

Process Options

18,01;Fourier mode: 3, 2

18,02;Fourier levels: 1e-08, 0.001, 0.5, 2

18,03;Fourier notch: 0, 0, 1, 1

18,04;Fourier notch freq: 1e+09, 1e+09, 1e-10, 0

18,05;Autocorrelate: 50, 0, 0, 0, 0, 0, 1, 1

18,06;

18,07;

18,08;

DSP stuff

19,08;DSP control: 290, 0, 0, 1, 1, 3, 3

19,09;c:\stm386\a.out

19,10;DSP offset: 0, 0, 0, 1e-06

19,11;DSP loop: 0.1, 1e-09, 1e-06, 100

19,12;DSP scan1: 1e-07, 1e-07, 0, 0, 1e-06, 0

19,13;DSP scan2: 0, 0, 0, 0, 1

19,14;DSP head: 5e-09, 5e-09, 1.5e-09, 0, 0, 0

19,15;DSP gain1: 1, 1, 1, 1, 1, 1

19,16;DSP gain2: 1, 1, 1e-09, 0

19,17;DSP jerk1: 1e-07, 1e-07, 0.0001, 0.01, 1e-09, 30

19,18;DSP jerk2: 50, 50, 1, 1, 0

19,19;DSP knob: 0, 0, 0, 0, 0, 0, 0, 0

19,20;DSP move: 0.5, 0.2, 5e-10, 1e-09, 0, 0.001, 1e-07

BIBLIOGRAPHY

- [1] G. Binning, H. Rohrer, C. Gerber and E. Weibel, Phys. Rev. Lett. **49** (1982) 57.
- [2] D.W. Abraham, H.J. Mamin, E. Ganz and J. Clarke, IBM J. Res. Develop. **30** (1986) 492.
- [3] E.J. van Loenen, D. Dijkkamp, A.J. Hoeven, J.M. Lenssinck and J. Dieleman, Appl. Phys. Lett. **55** (1989) 1312.
- [4] T.R. Albrecht, M.M. Dovek, M.D. Kirk, C.A. Lang and C.F. Quate, Appl. Phys. Lett. **55** (1989) 1727.
- [5] Y.Z. Li, L. Vazquez, R. Piner, R.P. Andreas and R. Reifenberger, Appl. Phys. Lett. **54** (1989) 1424.
- [6] J.P. Rabe and S. Buchholtz, Appl. Phys. Lett. **58** (1991) 702.
- [7] H.J. Mamim, S. Chiang, H. Birk, P.H. Guethner and D. Rugar, J. Vac. Sci. Technol. **B 9** (1991) 1398.
- [8] D.M. Eigler and E.K. Schweizer, Nature **344** (1990) 524.
- [9] J.A. Stroscio and E.M. Eigler, Science **254** (1991) 1319.
- [10-11] Jasprit Singh, in *Quantum Mechanics: Fundamentals and Applications to Technology* (John Wiley & Sons Incorporated, New York, 1997).
- [12] H.W Fink, IBM J. Res. Develop. **30** (1986) 264.
- [13] Y. Kuk and P.J. Silverman, Appl. Phys. Lett. **48** (1986) 125.

[14] T. Michely, K.H. Besocke and M. Teske, *J. Microscopy* **152** (1988) 299.

[15] C. Chen, *Introduction to Scanning Tunneling Microscopy* (John Wiley & Sons Incorporated, New York, 1993) 355.

[16] O.V. Eshbach and M. Souders, *Handbook of Engineering Fundamentals* (Wiley, New York, 1980).

[17] W. Haiss, J.K. Sass, D. Lackey and M. van Heel, Fritz-Haber-Institut der MPG, Faradayweg 4-6, D-14195 Berlin, Germany.

VITA

Paul G. Person was born on July 31, 1970 in Lockhart, Texas to Gustav and Marguerite Person. After completing his work at Navarro High School, Geronimo, Texas, in 1988, he entered Texas A&M University in College Station, Texas. In the fall of 1988, he transferred to Southwest Texas State University and later received his Bachelor of Science degree in Physics in the December 1997. In January 1998, he continued his education in the physics masters program at SWT. While in San Marcos, he received several awards: Dean's List, Academic Excellence, Excellence in Graduate Research, and Chi Sigma Chi Quake Tournament Champion.

Permanent address: 4301 FM 2623
Seguin, Texas 78155

This thesis was typed by Paul G. Person.